İSTANBUL TECHNICAL UNIVERSITY ★ INSTITUTE OF SCIENCE AND TECHNOLOGY

THE EFFECT OF BARRIER MATERIAL AND GETTER MATERIALS ON PRESSURE INCREASE OF VACUUM INSULATED SYSTEMS

M.Sc. Thesis by

Ayşe ÇELİK

Department : Polymer Science and Technology

Programme: Polymer Science and Technology

Supervisor : Prof. Dr. I.Ersin SERHATLI

MAY 2003

İSTANBUL TEKNİK ÜNİVERSİTESİ ★ FEN BİLİMLERİ ENSTİTÜSÜ

VAKUMLU YALITIM SİSTEMLERİNDE BARİYER MALZEMELER VE GETTER MALZEMESİNİN BASINÇ ARTIŞINA ETKİSİ

YÜKSEK LİSANS TEZİ

Ayşe ÇELİK

Anabilim Dalı: Polimer Bilim ve Teknolojisi

Programı: Polimer Bilim ve Teknolojisi
Tez Danışmanı: Prof. Dr. I. Ersin SERHATLI

MAYIS 2003

ACKNOWLEDGEMENTS

I would like to express my sincere gratitude to my thesis supervisor, Prof.Dr. Ersin Serhatlı for his supervision, extensive support and suggestions throughout my studies.
I would like to express my thanks to Arçelik A.Ş for invaluable support in the name of Turgut Soysal; Şemsettin Eksert and Doç.Dr. M. Yalçın Tanes.
I sincerely thank to Fatih Özkadı; Dr.Hande Güçlü and all the members of "Advanced Insulation Program" for their invaluable help and support. I would like to extend my thanks to all the members of Material Technologies Department in the name of Sibel Odabaş.
My greatest thank is to Esra Küçükpınar for her endless support and encouragement throughout the studies.
I would like to thank all the master students in Arçelik R&D Center.
I want also to thank Osman G. Ersoy, who supported me during the studies.
I thank also to my family who gave me support and encouragement throughout the years.

İstanbul, April, 2003 Ayşe ÇELİK

TABLE OF CONTENTS

LIST of ABBREVIATIONS

VIP	:Vacuum Insulation Panel
VIC	:Vacuum Insulation Component
XPS	:Open Celled Extruded Polystyrene
OCPU	:Open Celled Polyurethane
RUF	:Recycled Urethane Fluff
VACSIM	:Vacuum Simulation
WVTR	:Water Vapor Transmission Rate
PA	:Polyamide
PET	:Poly (Etyleneterephthalate)
EVOH	:Polyethylene Vinyl Alcohol
LLDPE	:Lineer Low Density Polyetylene
PP	:Polypropylene
RH	:Relative Humidity
ABS	:Acrylonitrile Butadien Styrene
HDPE	:High Density Polyetylene
HIPS	:High Impact Polystyrene
PMMA	:Polymethyl methacrylate
WS	:Styroblend
IG 1-IG 2	:Ionization Gages
CG1-CG2	:Capacitance Manometers
PM1-PM3	:Rotary Vane Pumps
TP1-TP2	:Turbomolecular Pumps
G	:Getter
NG	:No-getter

LIST of TABLES

LIST of FIGURES

LIST of SYMBOLS

Al	:Aluminum
W	:Amount of adsorbed gas
P	:Pressure
k	:Constant in Freundlich isoterm
$\mathbf{n_i}$	:Constant in Freundlich isoterm
θ	:Solid surface covered by gas molecules
θ **-1**	:Free surface on adsorbent
$\mathbf{r_a}$	:Adsorption rate due to Langmuir isoterm
$\mathbf{r_d}$	:Desorption rate due to Langmuir isoterm
K	:The division of r_a to r_d
S	:Solubility coefficient
D	:Diffusion coefficient
$\mathbf{E_a}$	:Activation energy
R	:Universal gas constant
$\mathbf{T_g}$	:Glass transition temperature
$\mathbf{S_t}$	:Kinetically adsorption rate
$\mathbf{P_1}$	:Probability that particle finds a free site
$\mathbf{P_2}$	:Probabillity that particle finds sufficient energy for adsorption
$\mathbf{P_3}$	:Probability that P_1 and P_2 are fulfilled
ν	:Collision frequency
$\mathbf{m_1}$	:Mass of the gas molecule
k	:Bolztman constant
T	:Temperature
$\mathbf{Q_0}$	:Total capacity at zero speed
$\mathbf{Q_1}$	:Capacity of getter at time t_1
$\mathbf{S_1}$	:Acceptable speed at time t_1
$\mathbf{Q_2}$	:Capacity of getter at time t_2
$\mathbf{S_2}$	:Acceptable speed at time t_2
Ar	:Argon
$\mathbf{H_2}$	:Hydrogen
$\mathbf{H_2O}$	:Water
$\mathbf{N_2}$	:Nitrogen
$\mathbf{O_2}$	:Oxygen
CO	:Carbonmonoxide
$\mathbf{CO_2}$	:Carbondioxide
Ba	:Barium
Ti	:Titanium
α	**:**Outgassing parameter
β	:Outgassing parameter
$\mathbf{P_i}$	:Partial pressure
$\mathbf{P_{init,i}}$	:Initial partial pressure for gas i
p	:Permeability coeeficient
A	:Area of barrier
Δ**P**	:Pressure difference between two sides of barrier
t	:Time

d	:Thickness of barrier
m_2	:Amount of water vapor diffused inside the panel
M_w	:Molecular weight
$g(t)$	:Outgassing rate at time t
g_0	:Amount of outgassed gas
V_{gas}	:Total volume of gas that is accumulated in insulation volume
V_{in}	:Volume of gas that is permeated from inner part of cabinet into the insulation volume
V_{out}	:Volume of gas that is permeated from outer part of cabinet into the insulation volume
Δp_0	:Pressure difference between outside pressure and the pressure inside the panel after evacuation process
P_{out}	:Pressure at outside conditions
P_{in}	:Pressure value in insulation volume after evacuation process
A_{out}	:Outside area of plastic barrier material
A_{in}	:Inside area of plastic barrier material
p_{out}	:Permeability of barrier material at outside temperature conditions
p_{in}	:Permeability of barrier material at inside temperature conditions
V	:Evacuated insulation volume
ΔP_n	:Pressure increase at the end of n^{th} time
ΔP_1	:Pressure increase at the end of first unit time
n	:mol number
t_{air}	:Measurement time for pressure increase due to gas permeation
t_{wv}	:Measurement time for pressure increase due to water vapor permeation
$P_{initial\text{-}air}$	:Pressure in insulation volume at the beginning due to air
$P_{initial\text{-}WV}$	:Pressure in insulation volume at the beginning due to water vapor
$P_{ff/frz\text{-}air}$	:Air pressure at the inside conditions of the cabinet
$P_{out\text{-}air}$	:Air pressure at outside conditions
$P_{ff/frz\text{-}WV}$	:Water vapor pressure at the inside conditions of the cabinet
$P_{out\text{-}WV}$	:Water vapor pressure at outside conditions
T_{in}	:Inside temperature of cabinet
T_{out}	:Outside temperature
$BaLi_4$	:Barium-Lithium alloy
Co_3O_4	:Cobaltoxide
CaO	:Calciumoxide
σ	:Sigma bond length
ε	:Potential energy constant
εk	:Lennard-Jones temperature

THE EFFECT OF BARRIER MATERIALS AND GETTER MATERIAL ON PRESSURE INCREASE OF VACUUM INSULATED SYSTEMS

SUMMARY

Increasing ecological concerns and new energy regulations are forcing the refrigeration appliance manufacturers to the reduction of energy consumption. This can be achieved by enhancing the refrigeration system or the insulation system of the appliance. The utilization of vacuum insulation systems in the refrigeration appliances seems to be a promising solution for the reduction of energy consumption.

Vacuum insulation technology is based on placing an inner filler material within a barrier material and evacuating the air from the inside. This technology finds two applications; vacuum insulated panels (VIPs) and vacuum insulated cabinets (VICs). VIPs are manufactured by wrapping an inner filler material and an absorbent material in a barrier. Then the panel is evacuated and sealed to the atmosphere. The usage of the absorbent is necessary to collect the gases accumulated in the panel during its lifetime. VICs are manufactured by filling the evacuated inner filler material in a multilayer plastic cabinet and then sealing it to maintain the vacuum level constant. Homogenous insulation can be achieved by this technology.

The studies in this thesis can be grouped in two sections. In the first part, the components in VIP concept were investigated. The absorption characteristic of absorbent material for various gases was experimentally determined. Three different absorbent materials were experimentally investigated due to their absorption properties and they were compared to each other. The chemical ingredients of studied absorbents were same with different amounts. So, the effect of ingredients amount on absorption performance was determined. By the evaluation of experimental results in a vacuum simulation program (VACSIM) pressure increase at the end of specified time duration was predicted. VACSIM simulation results were compared to experimental results to check the reliability of theoretical calculations.

In the second part of the thesis, the pressure increase in the insulation volume of a VIC cabinet was simulated by VACSIM simulation program for three different systems. In System-1, simulations were made for the “freshfood” part of refrigerator, where the conditions are, outside: 25^0C& 50% RH, inside: 5^0 C& 50% RH. It was studied on 14 different multilayer structures to determine the best one. Best structure causes minimum pressure increase in the insulation volume. The pressure increase in insulation volume cannot exceed the critical pressure value of inner filler material, that is why optimum thickness of the best structure was determined. If the critical pressure was exceeded the insulation performance of the vacuum insulated cabinet will be deteriorated. In System-2 simulations were made for the “freezer“ part of refrigerator, where the conditions are, outside: 25^0C&50% RH, inside: -18^0C& 50% RH. Again determination of best structure and thickness optimizations were made for this system. In System-3 simulations were made for ambient conditions, where both inner and outer conditions are assumed as 25^0C& 50% RH. The aim of last simulation was the comparison of simulation results to experimental results and checking the reliability of VACSIM program.

As a consequence of this study, the chemical ingredient amount of tested absorbent materials was found ineffective on absorption capacity for 10 years. Three absorbent materials were tested due to their absorption speed and capacity and it was determined that they can be used in VIPs. According to the simulations, the usage of absorbent material in VIPs was determined as essential. Simulation results were compared to experimental results and they were observed good in correlation. So this program can be used to predict vacuum level in any system for desired time duration. By using VACSIM program the best barrier structure for VIC concept was determined as ABS+EVOH for both freshfood and freezer parts of refrigerator. After determination of best barrier structure, thickness optimization was made for this structure:

- System-1: It was studied on 13 different thicknesses of the best structure. The most effective was found as; outer structure: 3mm ABS+0.6mm EVOH; inner structure: 1.8 mm ABS+0.6 mm EVOH. By using this structure total pressure increase in insulation volume was predicted as 93 mbar at the end of 10 years.
- System-2: It was studied on 11 different thicknesses of the best structure. The most effective was found as; outer structure: 3mm ABS+0.5mm EVOH; inner structure: 1.4 mm ABS+0.4 mm EVOH. By using this structure total pressure increase in insulation volume was predicted as 95 mbar at the end of 10 years.

By System–3 simulation, theoretical calculations were compared to experimental results, so the reliability of VACSIM-VIC program was checked, the results seemed good in correlation.

VAKUMLU YALITIM SİSTEMLERİNDE BARİYER MALZEMELER VE GETTER MALZEMESİNİN BASINÇ ARTIŞINA ETKİSİ

ÖZET

Çevresel sorunların her geçen gün artması ve yenilenen enerji regülasyonları nedeniyle beyaz eşya üreticileri, ürünlerinde enerji tüketimini azaltmaya yönelik teknolojik çözüm arayışlarına hız vermiştir. Bu çözümleme, soğutucu ürünlerde soğutma sistemi ve yalıtımın iyileştirilmesi ile mümkün olmaktadır. Yalıtımın iyileştirilmesi amacı ile buzdolaplarında vakumlu yalıtım teknolojisi kullanılmasının enerji tüketimini azaltmaya yönelik umut vaat eden bir çözüm olduğu görülmektedir.

Vakumlu yalıtım teknolojileri, açık hücreli bir iç dolgu malzemesinin bariyer malzeme içerisine konularak vakumlanması ve ardından vakum sızdırmayacak şekilde kapatılmasına dayanmaktadır. Bu teknolojinin vakumlu yalıtım paneli (VIP) ve vakumlu yalıtım kabini (VIC) olmak üzere iki farklı uygulaması bulunmaktadır. VIP' ler, iç dolgu malzemesi ile adsorbant malzemesinin, film formundaki bariyer malzemenin içerisine yerleştirilmesi, vakumlanması ve vakuma dayanacak şekilde kapatılması ile elde edilir. VIC' ler ise çok katlı plastik bariyer malzeme içerisine vakumlanmış iç dolgu malzemesinin yerleştirilmesi ve ardından vakuma dayanacak şekilde kapatılması ile elde edilmektedir. Bu sayede buzdolabında homojen yalıtım sağlanır.

Bu tez kapsamında yapılan çalışmalar iki gruba ayrılabilir. İlk kısımda, VIP lerde kullanılan absorbant malzemelerin gaz tutma hızları ve kapasiteleri deneysel olarak incelenmiş, üç farklı absorbant malzemenin absorpsiyon özellikleri birbirleriyle karşılaştırılmıştır. İncelenen absorbantlar aynı kimyasal içeriğe sahip olup bu kimyasalların miktarları farklıdır. Bu sayede, kimyasal miktarının absorbsiyon performansına etkisi belirlenmiştir. Elde edilen deneysel sonuçların vakum simülasyon programında (VACSIM) değerlendirilmesi ile panel içerisinde belirli süre sonunda oluşacak basınç artışı teorik olarak hesaplanmıştır. Belirli süre zarfında, çeşitli VIP' lerin panel iç basınçlarındaki artış, spirotorr cihazı ile deneysel olarak ölçülmüş ve sonuçlar, VACSIM programı sonucu elde edilen teorik sonuçlarla karşılaştırılmıştır. Bu sayede VACSIM programının güvenilirliği test edilmiştir.

Tezin ikinci kısmında, VACSIM simülasyon programının VIC' ler için geliştirilmiş kısmı kullanılarak, farklı çok katlı plastik yapıların bariyer malzeme olarak kullanılması durumunda, VIC' nin yalıtım hacminde belirli süre sonunda oluşacak basınç artışı teorik olarak belirlenmiştir Hesaplamalar farklı ortam şartlarını temsil eden üç farklı sistem için yapılmıştır: Sistem-1 buzdolabının sebzelik kısmını temsil etmekte olup kabin içi : 5^0 C ve 50% bağıl nem; kabin dışı: 25^0C ve 50% bağıl nem olarak kabul edilmiştir. Bu sistemde 14 farklı yapı üzerinde çalışılarak gaz geçirgenliği en düşük olan çok katlı yapı en iyi yapı olarak bulunmuştur. Yalıtım hacminde oluşacak basınç artışı, iç dolgu malzemesinin kritik basıncını geçerse yalıtım özelliği bozulmaktadır. Bu nedenle belirlenen en iyi yapı için en uygun kalınlık, yapılan simülasyonlar ile tespit edilmiştir. Sistem-2, buzdolabı dondurucu bölgesini temsil etmektedir; kabin içi: -18^0C ve 50% RH; kabin dışı: 25^0C ve 50% kabul edilmiştir. Sistem–1 için yapılan, en iyi yapının ve ardından en uygun kalınlığın belirlenmesi çalışmaları Sistem-2 için yine 14 farklı yapı üzerinde yapılmıştır.

Sistem-3 simülasyonu ortam şartlarını temsil etmektedir, hem kabin içi hem de kabin dışı 25^0C ve 50% bağıl nem olarak hesaplamalarda kullanılmıştır. Bu çalışmanın amacı, ortam şartlarında deneysel olarak ölçülen vakum seviyesi sonuçlarını VACSIM sonuçları ile karşılaştırarak simülasyon programının güvenilirliğini test etmektir.

Çalışmanın sonunda, VIP lerde kullanılabilecek test edilen absorbant malzemelerin kimyasal içerik miktarının 10 yıllık süre zarfında absorpsiyon kapasitesi üzerinde etkin olmadığı belirlenmiştir. Üç farklı absorbant malzemenin absorpsiyon hızı ve kapasitesi deneysel olarak incelenmiş, bu malzemelerin VIP lerde kullanımın uygun olduğu görülmüştür. Gerek yapılan simülasyonlar, gerekse deneysel çalışmalar sonucunda VIP' lerde absorbant kullanımın zorunlu olduğu bulunmuştur. Simülasyon sonuçları deneysel sonuçlar ile karşılaştırılmış, sonuçların uyum içerisinde olduğu görülmüştür. VIC konsepti için geçirgenlik nedeni ile buzdolabının yalıtım hacminde en az basınç artışına neden olan yapı ABS+EVOH olarak belirlenmiştir. En iyi yapı belirlendikten sonra farklı kalınlıktaki yapılar için kalınlık optimizasyonu yapılmıştır:

- Sistem-1: En iyi yapının 13 farklı kalınlığı üzerinde çalışılmış, en uygun kalınlığın: dış plastik: 3mm ABS+0.6mm EVOH; iç plastik: 1.8 mm ABS+0.6 mm EVOH olduğu bulunmuştur. Bu yapı kullanıldığında 10 yıl sonunda yalıtım hacminde oluşacak basınç artışı 93 mbar olarak hesaplanmıştır.
- Sistem-2: En iyi yapının 11 farklı kalınlığı üzerinde çalışılmış, en uygun kalınlığın dış plastik: 3mm ABS+0.5mm EVOH; iç plastik: 1.4 mm ABS+0.4 mm EVOH olduğu bulunmuştur. Bu yapı kullanıldığında 10 yıl sonunda yalıtım hacminde oluşacak basınç artışı 95 mbar olarak bulunmuştur.

Yapılan üçüncü simülasyon ile elde edilen teorik hesaplama sonuçları deneysel sonuçlarla karşılaştırılmış ve VACSIM programının güvenilirliği test edilmiştir.

1. INTRODUCTION

Increasing ecological concerns and new energy regulations are forcing the refrigeration appliance manufacturers to the reduction of energy consumption. Advanced vacuum insulation technologies, including vacuum insulation panels (VIP) and vacuum insulated components (VIC) seem to be promising solutions to achieve reduced energy consumption.

The insulation effectiveness of VIPs and VICs is very good compared to conventional polyurethane insulation in refrigerators. They allow significant amount of energy saving during refrigerator life and result in increased available inner volume in appliances. A VIP is manufactured by packing inner filler materials such as fiberglass, silica, perlite, aerogel, open celled extruded polystyrene (XPS), open celled polyurethane (OCPU), recycled urethane fluff (RUF) and chemical absorbents, called getter, in a film like laminated plastic barrier or stainless steel, as in Figure 1.1 [1]. After manufacture air is evacuated from the inside of the panel and it is sealed to keep vacuum level as constant. Vacuum level depends on the selected inner filler material. Generally applied pressures are changing between 10^{-2}-10 mbar. Since the thermal conductivity is low, evacuated insulator has the ability to reduce heat transmission from the ambient to the inner volume of the refrigerator. VIP's are used in refrigerator insulation by placing them between inner and outer walls of the refrigerator or freezer [2].

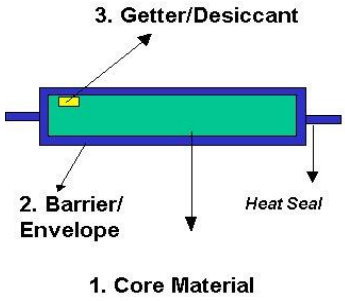

Figure 1.1: Schematic structure of VIP

Application of VIC is different than VIP's. A VIC is performed by, filling a cabinet and a door with an insulating material. The material is then evacuated and sealed to maintain the vacuum level as constant. A schematic structure of VIC is given in Figure 1.2 [3].

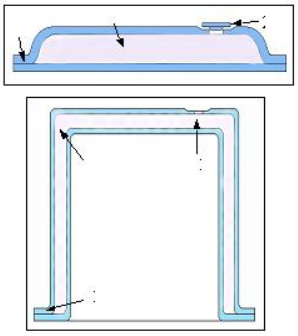

Figure 1.2: Schematic structure of VIC

As a result of their low thermal conductivity, the usage of VIP or VIC is necessary to reduce heat transmission from the ambient to the inner volume of refrigerator. However it is very difficult to keep the vacuum at a constant level. For VIP-VIC concepts in a period of 10-15 years, the gas sources will degrade the vacuum level. The gas sources in panel or cabinet caused by gas and vapor diffusion from barrier material and outgassing from inner filler material. This degradation results in diminishing of the heat insulating property of the evacuated vacuum insulation component. To prevent this effect, absorbent materials, called getters should be used. These materials are able to absorb water vapor and gases that were accumulated in the panel and/or cabinet during its lifetime.

Insulation performance of a VIP or VIC maintains until vacuum level inside the panel or cabinet reaches to the critical pressure value of inner filler material. Below the critical pressure value of inner filler material, thermal conductivity is independent of pressure. At this threshold pressure the thermal conductivity starts to increase, therefore it is critical to keep the pressure value below that threshold pressure [3].

In this thesis, the permeability affect of barrier material on insulation performance was determined and getter materials, which are being used in VIPs were fully characterized. The vacuum levels of different VIP's were measured due to time and experimental results were compared with theoretical calculations that were calculated by VACSIM-VIP simulation program. The affect of barrier material structure and the thickness on vacuum level change, were also evaluated by VACSIM-VIC simulation program and the results were compared with experimental results. The best possible multilayer structure for a barrier material that would decrease water vapor and gas permeation into the insulation volume is determined as the best structure in terms of its thickness and structure.

2. THEORETICAL PART

2.1. Permeation Theory

Two significant properties derived from Fick's first law can be measured to estimate the barrier properties of plastic films and similar materials. These properties are the gas permeability and the water vapor transmission rate. Transport of gases and water vapor through barrier structures occurs in three main steps [4].

1- Solution of penetrate on the surface of the material 2- Diffusion of penetrate through material according to the concentration difference. 3- Desorption from the other side.

Permeability can be given by equation 2.1, where D is the diffusion coefficient and S is the solubility coefficient [4].

$$P=D\,S \tag{2.1}$$

The major factors affecting barrier permeability are given below:

- Temperature
- The size of permeating molecule
- Cavities on the structure of polymer
- Pressure, relative humidity and concentration differences
- Structure of polymer

Both D and S values are changing by the temperature. Permeability increases, as temperature increases. The relationship between temperature and permeability coefficient is given by Arrhenius equation, as in equation 2.2 [5].

$$P = P_0 \exp\left(\frac{-E_a}{RT}\right) \tag{2.2}$$

In equation 2.6, P_0 represents permeability constant, E_a is the activation energy, R is universal gas constant and T (^{0}K) is the temperature.

Absorbed water can cause an increase in permeability by softening the material, so in many cases the permeability of material is changing by relative humidity of environmental conditons. Therefore relative humidity is important to calculate the permeability value.

Diffusion along a polymer occurs by transport of small molecules through the cavities between polymer chains and through other free volumes in the structure. That is why permeating rate relates mostly to the size of penetrant molecules and the size of the cavities in the barrier structure. Small molecules can diffuse easier than the big ones although they have same solubility coefficient. As an example, the size of O_2 molecule is bigger than water and permeation of O_2 through vacuum coated barrier layers occurs only through macroscopic defects in the range of 0.1 μm, where the permeation of water vapor occurs also through microstructure scales. Physical properties, such as amorphous or crystalline structure of polymer, strongly affect the size of the free volumes in the polymer structure that are important for diffusion [4].

Amorphous structure: Polymers are in amorphous state at the temperatures over T_g value. At this state polymer chain moves freely and there occurs substantial amount of free volumes in the structure. So, the small molecules permeate easily through these free volumes, and permeance rate will be higher.

Crystalline structure: Under T_g value polymers are in crystalline form and the movement of molecules is difficult and the amount of free volume on the structure decreases. Crystalline structures are tend to molecular packaging and they can be considered as impermeable. But it should be take in consideration that there is not a structure with 100% crystallinity, there is always an amorphous part in crystalline structure and permeation occurs through this amorphous part. As a result, crystalline polymers resist to permeation more than the amorphous ones. Other structural properties of polymer, affecting permeability are given below:

- Polarity of polymer
- Rigidity of polymer chain
- Inert against penetrant
- Linking and interaction between chains
- High Tg value
- Molecular symetry, crystallinity and orientation

Due to the polarity of polymer structures, polymers which have good barrier properties against gases are poor barriers for water vapor. Polymers containing

hydroxyl groups with high polarity (polyvinylalcohol, cellulose etc.) are good barriers against gases [6]. Polymers, containing polar groups can absorb moisture from environment or from a liquid that is in contact with polymer and this reduces barrier effect. Non-polar hydrocarbon polymers, like polyethylene, are good barrier against water vapor where they are poor barrier against gases [4]. In Table 2.1, permeability values of some of the known polymers with different polarities are given.

Table 2.1: Water Vapor Permeability at 25^0C and 50% Relative Humidity [4]

Film	$P = \frac{(cm^3)(mm\ x10^8)}{(cm^2\ s)(cm\ Hg)}$
Poly (vinyliedene chloride) (Saran)	0.3-1.0
Polytetrafluoroethylene (Teflon)	0.3
Butyl rubber	1.3
Polyethylene (density 0.960)	1.2
Polyethylene (density 0.938)	2.5
Polyethylene (density 0.922)	9.0
Polypropylene (density 0.907)	5.1
Poly (vinylchloride)	6.1
Poly (vinylchloride- vinyl acetate)	7.0
Poly (ethylene terephthalate) (Mylar)	13
Polystyrene	12
Polyacrylonitrile	13
Polybutadiene	47
Poly (styrene-butadiene)	9
Poly (butadiene-acrylonitrile) (62%)	15
Polyisoprene (natural rubber)	30
Polyamide (nylon 66) (95% relative humidity)	68
Cellulose acetate	550
Cellulose acetate (15% dibutyl phthalate)	740
Ethyl cellulose, plasticised	1300
Poly (vinyl alcohol), p=2.3 cm Hg	4200

2.1.1. Usage of Barrier Materials in VIPs

Gas permeation through the barrier envelope is one of the most important contribution for the pressure increase in a vacuum panel during its life. Depending on the structure and materials of the barrier film, gas and water vapor inlet can take place through the whole surface of the barrier or through the edges of the barrier or both. This penetration affects the insulation performance of panel. That is why permeability of barrier material should be characterized. Several types of barrier materials, having different structures and degrees of permeability are available for plastic panel applications. Multilayer structures are very effective to decrease gas and water vapor permeability of films. They can be either multilayer plastics, metallized plastic, and/or metal folio/plastic composite films.

A multilayer barrier consists of typically from the layers given below [5,6]:

- Film layer for mechanical strength (PA)
- Film layer with low permeability values (metallized PET, EVOH, LLDPE)
- Metal folio layer to be barrier against permeation (Al)
- Film layer for hot welding (PE, PE/PP)

The most effective barrier properties are seen by the structures containing Al layer. Barrier effectiveness of the structures increase by the order shown below:

With metal folio (Al)> With metalized folio> Without any metal folio

In multilayer structures, metal folio-Al layer that is placed between plastic layers represents very effective barrier properties compared to other structures. Diffusion in Al containing structures occurs through pinholes on Al. A schematic structure of this mechanism is shown in Figure 2.1 by comparing the diffusion mechanism through multilayer films without a metal layer [4].

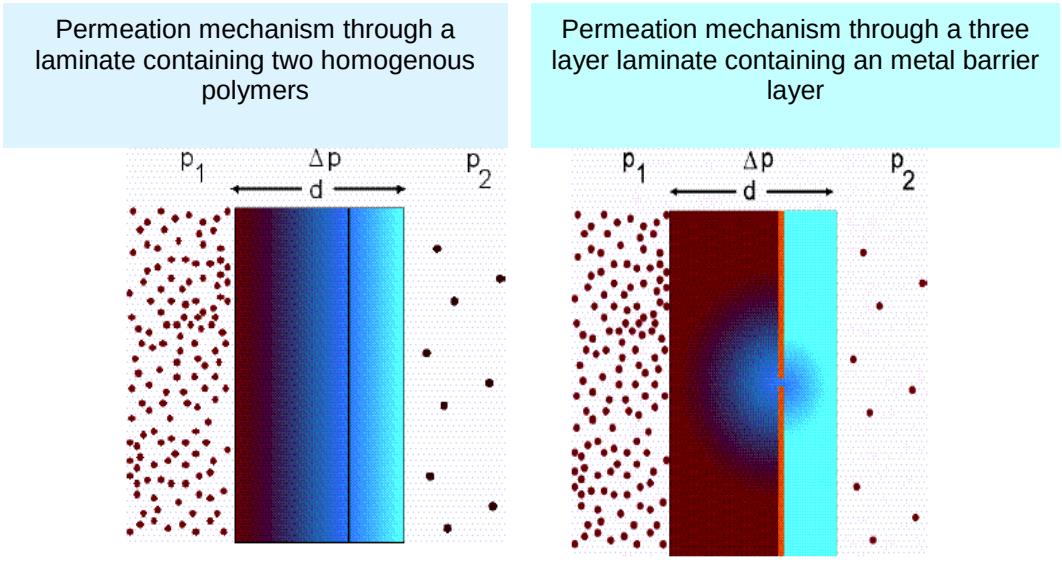

Figure 2.1: Diffusion mechanisms through structures with or without a metal layer

The lowest permeability values can be observed, when metal folio and metallized film are used together in a multilayer structure. In this case, pinholes on the metal folio are masked by metallized layer, so barrier effect against permeation will be increased [4].

2.2. Inner Filler Material

Vacuum insulated panels (VIPs) have thermal conductivity 3 to 7 times lower than conventional insulating materials such as closed cell polyurethane and polystyrene

foams or fiber glass, as showed in the Figure 2.2. The most important parameter in a vacuum insulation system is the critical pressure value of inner filler material. The critical pressure of the material is the critical vacuum level of the material above which the thermal conductivity of the vacuum panel increases rapidly. Hence, the selection of inner filler material is one of the most important factors in the characterization of the vacuum insulation. Thermal conductivity is independent from pressure and stay as constant until to reach critical pressure value. As pressure increases, the amount of gas molecules in the panel will increase and mean free path of the gases will shorten. When the distance of mean free path will be equal to the cell size of inner filler material, the pressure reaches to critical pressure and thermal conductivity increases with pressure. Pressure increase can reach to critical pressure and surpass it in a few years, so heat insulation property of vacuum system degrades [7].

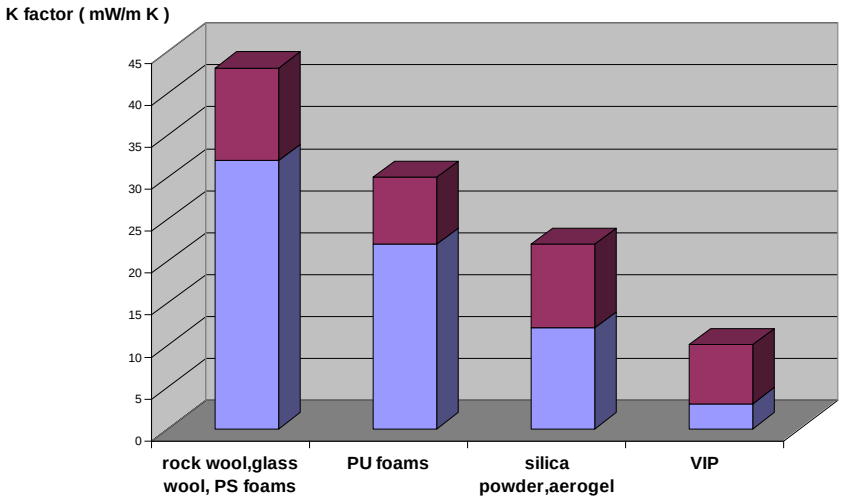

Figure 2.2: Comparison of different insulation materials

2.3. Getter Material

After VIP is manufactured, it is very difficult to keep vacuum level as constant, because of the permeation through barrier material and outgassing from inner filler material. To prevent the pressure increase inside the panel absorbent materials should be used. These materials are known as getter. The use of getters in vacuum technology has gained an increasing interest, and the development of this type of pump for new and advanced applications. Working of getter materials are related to surface and bulk characteristics of metals and gas-surface interaction phenomena [8].

When gas molecules interact with a solid surface, several phenomena can take place. The following ones are shown in Figure 2.3, and their description can be given as below [8]:

- Adsorption: Capture of molecules by the surface
- Desorption: Emission of molecules from the surface
- Backscattering: Bounching back of molecules that effects the surface
- Diffusion: Penetration of adsorbed atoms from the surface into the solid bulk or movement of dissolved atoms from the solid bulk to the surface.
- Displacement: Displacement of an adsorbed molecule by another effective molecule.
- Surface reactions: Formation of new molecules at the surface from adsorbed molecules of different species.

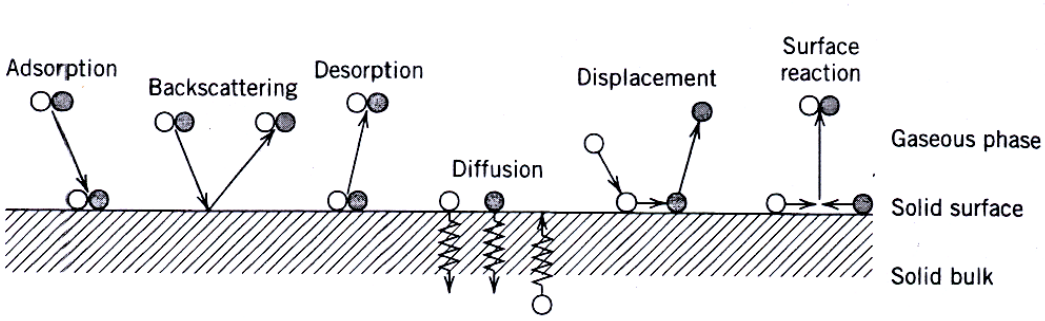

Figure 2.3: Types of gas - surface interactions

Some of these phenomena tend to remove molecules from the gaseous phase, however others tend to remove molecules into the gaseous phase. If the surface has suitable characteristics, the adsorption phenomena can, however prevail (together with diffusion into the bulk, under certain conditions of temperature) in a vacuum system.

Adsorption is related to temperature, pressure and interaction potential between adsorbat and adsorbent, as in equation 2.3 [9].

$$W = F(P, T, E) \tag{2.3}$$

The graph of W-P gives the adsorption isoterm[1] of gas-solid interface. One of the isoterms, known as Freundlich isoterm, defines the relationship between the amount

[1] Adsorption isoterm is described as the relationship between the amount of adsorbed gas by adsorbant and the equilibrium pressure at constant temperature [8].

of adsorbed gas (W) and pressure (P) as shown in equation 2.4, where k and n are constants.

$$W = kP^{1/n} \tag{2.4}$$

Another isoterm about the adsorption of gas on solid material is Langmuir isoterm. The theory is related to the adsorption-desorption kinetic of gas molecules on solid surface. The solid surface covered by gas molecules is represented by θ and free surface at any time can be given by $(\theta - 1)$. Adsorption rate (r_a) and desorption rate (r_d) can be calculated related to the equations 2.5.a and 2.5 b, k_d is desorption reaction rate and k_a is the reaction rate due to the rate of striking of molecules to the surface, which belongs to the pressure [9].

$$r_d = k_d\theta \tag{2.5 a}$$

$$r_a = k_aP(1-\theta) \tag{2.5 b}$$

In equilibrium state r_a and r_d are equal to each other and Langmuir isoterm changes as in equation 2.6. K represents the ratio of adsorption rate to desorption rate ($K=k_a/k_d$)

$$\theta = \frac{k_aP}{k_d + k_aP} = \frac{KP}{1+KP} \tag{2.6}$$

Langmuir isoterm is more effective than Freundlich isoterm, to explain monolayer adsorption cases. At low pressures and weak adsorption cases, adsorption increases proportionally with pressure, because θ =KP and KP<<1. In this case, the surface will be covered completely by monolayer gas molecules, therefore pressure increase will not affect the amount of adsorbed gas. Getters used in vacuum isolation panels show the characteristics of Langmuir isoterms [9].

If the specified amount of test gas is sent on a solid and the volume is isolated, it will be observed decrease in gas pressure that is caused by the removal of molecules from the gaseous phase. This phenomena is usually known as gettering, and solid materials which exhibit this gettering capability are named as getter. The term getter is adopted when the capture of gaseous molecules is due to relatively strong forces like chemical bonds, and it refers to special metals both in pure or in alloy form. In this case, chemisorption takes place, so getters are also called as chemical pumps. Other materials such as molecular sieves, active charcoal, and so on, exhibit

adsorption of gas molecules; however, the forces involved are relatively weak and these materials, therefore, usually known as physical adsorbers rather than getters. In this case physisorption takes place [8].

The lattice structure can influence the gettering properties of a metal, in terms of diffusivity and solubility for gases. The gettering properties are however, firstly related to the surface characteristics of metals. The situation in the bulk of a metal, where each atom is completely surrounded by other metal atoms and has saturated bonds, is quite different from that at the surface. In fact, the surface atoms have a smaller coordination number[2] depends on the face of the crystal structure exposed at the surface. This means that the surface atoms have unsaturated bonds, which determine their reactivity versus the gas atoms or molecules colliding with the surface. The adsorption of gas molecules tends to saturate these free bonds and to reestablish the symmetry to which the atoms would be submitted if they were in the bulk of the crystal.

In gettering not only pure metals are used, but often also alloys are very important to achieve special properties. Metals and alloys are likely more frequently polycrystalline than monocrystalline. The grains consist of atoms arranged in a lattice with a precise space orientation. Adjacent grains have the same crystallographic structure, typical of the element considered, but the orientation is different. Therefore, in the space between two adjacent grains, there is a transition in the crystal orientation. This area, called grain boundary has an important influence on the metal properties, also from the point of view gettering. The grain boundary, in fact, is a zone of the metal where there is a lower density and a smaller coordination number in comparison with the bulk. The grain boundary atoms can, therefore, tend to react with foreign atoms; diffusion can also take place more easily than in the crystal bulk. Dimensions and shape of the grains can change during time, depending on temperature [8].

2.3.1. Adsorption and Desorption

Chemisorption can be dissociative, so that the individual atoms of the split molecules such as N_2, O_2, CO are actually bonded to the surface in the so called adsorption sites and can eventually diffuse into the bulk of the getter material if enough energy is provided. Chemisorption is usually irreversible in usual working conditions. However, in physisorption, the process is nondissociative and reversible [8].

[2] Coordination number: The number of ligands bonded to central metal atom. It is mostly between 2 and 12.

Kinetically, the adsorption process can be described by the following general equation 2.7:

$$S=P_1P_2P_3 \quad (2.7)$$

Where S is the rate of adsorption, P_1 is the probability that the particle colliding with the surface finds a free site, P_2 is the probability that the particle has sufficient energy for the adsorption to take place, P_3 is the probability, when the two above conditions are fulfilled the particle is actually adsorped, and ν is the collision frequency of the particle on the surface. The equation, $S= P_1P_2P_3$ is usually called sticking probability or sticking coefficient and depends on the surface coverage, the size of the adsorbate, the dissociative or nondissociative character of the adsorption and activation energy. The adsorption rate per unit time and unit area can be given by the equation 2.8, which also represents the basic expression for the gettering speed:

$$S=sp/(2\pi kT)^{1/2} \quad (2.8)$$

“p” is the gas pressure, m is the mass of the gas molecule, k is the Boltzmann constant[3], and T is the temperature in Kelvin unit. From the experimental data for S, it is then possible to derive the sticking probability values [8].

Some of the several factors related to the effectiveness for chemisorption of gases on metals are electronic factor, geometric factor, and the effect of impurities and imperfections. Since chemisorption implies the formation of a covalent bond, the electronic factor is very important. In this respect, the electronic properties of the d character metals are favorable to chemisorption for many gas molecules. As a result, getter materials are selected among metals with d characters. The possibility to accommodate molecules in the chemisorbed state also depends on the geometric characteristics of the metal that is on the relative distances of the surface metal atoms and the atom surface density. Different exposed crystal planes of the same metal can exhibit different chemisorption capabilities. Impurities and imperfections may promote or inhibit chemisorption and are sometimes responsible for unexpected changes in chemisorption properties of the same metal.

After adsorption, molecules can be reemitted and this phenomenon depends on the given energy. The physisorbed molecules can be easily desorbed, for example by heating, since the bond energies involved are relatively small. The release of

[3] Boltzman constant:The ratio of ideal gas constant to avogadro number

chemisorbed molecules implies the preliminary recombination of the component atoms and then the emission of the molecules. The energy involved in this process is large, and therefore desorption is generally very difficult by chemisorption [8].

2.3.2. Bulk Phenomena

The chemisorbed species can diffuse from the surface into the bulk of the getter material, depending on the nature of the diffusing species and the physicochemical characteristics of the sorbing material. The chemisorbed gas molecules at the surface have to break the chemical bonds with the adsorbing material, to diffuse into the bulk. The driving force for the diffusion is then the concentration gradient of the considered element, provided that enough energy is supplied. In this situation two processes, adsorption and diffusion proceed simultaneous [1]. Bulk diffusion occurs lastly, this stage is slower and therefore accounts for the part of the sorption curves with lower speed and higher capacity. The sorption stages are shown schematically in Figure 2.4 [8].

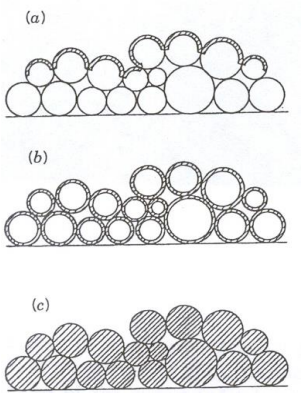

Figure 2.4: Different stages of gas sorption on a Ba film a) Surface diffusion b) İnternal surface diffusion c) Bulk diffusion

The first basic characteristics for a getter material are chemical affinity with gases and bulk diffusivity; first one is particularly important in determining the chemisorption of the gas species to be removed in a vacuum system, and the second allows the displacement of the adsorbate into the bulk of the getter material. Another basic characteristic is related to the possibility of achieving large surface areas. That is why getters are made up of alloys rather than of pure metals. Other important parameters to selecting a practical getter material are workability (possibility to transform the original getter material into powder to ensure enough surface area), hardness, safety (related to possible toxicity, pyroforicity and exothermic reactions with ambient or process gases and materials), stability under usual or specific storage conditions, availability, and cost all have to be taken into consideration.

2.3.3. Sorption Speed and Sorption Capacity

The gettering properties are evaluated by gettering speed and gettering capacity. The net removal rate of molecules from the gaseous phase as a result of the various possible interactions with the getter material is defined as sorption speed of getter material. This removal of molecules can be due to adsorption combined or not with adsorption. The sorption speed can be expressed in m^3*s^{-1}, $liter*s^{-1}$, or other convenient units. Multiplying the sorption speed by the pressure, the sorption throughput is calculated, which is given in $Pa*m^3*s^{-1}$, $torr*l*s^{-1}$ or other convenient units.

The gettering capacity (sorption capacity) is is the number of atoms or molecules that can be captured by the getter before it stops adsorbing gas. It is measured in $Pa*m^3$, mbar*liter, torr*liter or other convenient units. The sorption characteristics of a getter are represented by the sorption speed as a function of the sorbed quantity. Figure 2.5 shows the typical trend of the curve; Q_0 represents the total capacity at zero speed. This quantity corresponds to the amount of gas saturating on the surface, which occurs when getters work at room temperature. Q_0 corresponds to the maximum possible amount of gas sorbed, if diffusion takes place. The useful capacity of the getter is the amount of gas sorbed until the speed reaches the minimum acceptable value for the application. In Figure 2.5, the capacity of getter is Q_1, if S_1 is the acceptable speed; it is Q_2, if the acceptable sorption speed is S_2. These values of the sorption capacity are therefore so-called practical capabilities and can vary from situation to situation. ASTM F 798 defines a terminal gettering rate of a non-evaporable getter when the getter has sorbed an amount of gas corresponding to a decrease of the sorption speed to 5% of its initial value; the initial value is defined as the value measured after 3 minutes from the start of the sorption test. The sorption speed of a getter decrease with respect to time depending on working temperature and pressure conditions. If a getter is operating at high temperatures, its speed generally increases [8].

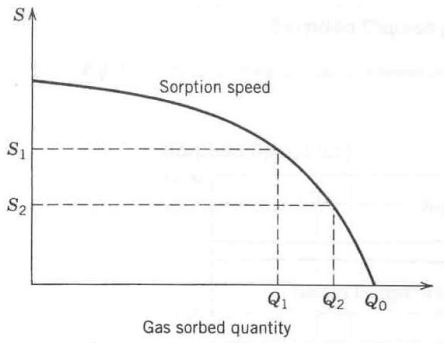

Figure 2.5: Typical sorption curve for a getter material

2.3.4. Working Conditions of Getter Materials

Getter materials are classified as evaporable and non-evaporable getters in two major groups. Non-evaporated getters are also called bulk or volume or massive getters. In the case of non-evaporable getters, there is no evaporation or sublimation of the getter material; the gases react on the available surface of the material and if sufficient energy is supplied, diffuse into the bulk [9].

Most commonly used evaporable getter types are Ba and Ti getters. Pure Ba is not used as such, because of its reactivity in air, which not allow its practical handling on a large scale. At first stage, in Ba getter developments getter consisting in a mixture of barium strontium carbonate sprayed on a tantalum strip, so called reactive getter was studied. Further developments led to use of various types of Ba containing alloys and to the stabilization of Ba by alloying with Al [9].

Zirconium based non-evaporable getter alloys are widely used in vacuum applications. But they can not be used in plastic evacuated panels due to their limited sorption capacity at room temperature and their necessity at high temperature heat activation prior their usage [9].

Other physical absorbents like molecular sieves, zeolites or activated charcoal are effective on adsorption of H_2O and some organic gases. But they show very weak sorption against N_2, O_2, H_2 and CO under vacuum application conditions. Their adsorption characteristic also changes according to the temperature which is another drawback of their usage [1].

2.3.5. Usage of Getters in VIPs

Several gas sources contribute to the pressure increase in the VIP during its life, i.e. residual gases left in the panel after the evacuation and sealing processes, gas diffusion from the inner filler material and gas permeation into the panel. These are deteriorating the vacuum level and isolation feature of VIP is damaged. The wide spectrum of gases present in a VIP, including H_2O, N_2, O_2, CO, CO_2, H_2, traces of blowing agents calls for a gettering system having huge sorption capacity and adequate sorption speed for all this gases. Getter provides substantial contributions in a VIP during the following stages [21]:

- Process: It can reduce evacuation time in a VIP by absorbing extra gases left in the panel.
- Initial life: Getter efficiently adsorbs residual gases left in the panel at the end of the evacuation process and those released during the foaming process in

the cabinet. The thermal conductivity value for the panel is therefore good from the very beginning of its life.

- Lifetime: Permeating and outgassed species, which can significantly increase the pressure are fixed by the getter.

2.4. Vacuum Simulation

Pressure increase in insulation volume of a VIP or VIC results in deterioration of insulation performance. That is why gas and water vapor permeation through barrier material, outgassing from inner filler material and capacity of getter system in a vacuum insulation component should be investigated. The effects of these components are evaluated by a software program, which is called Vacuum Simulation (VACSIM). VACSIM was developed for the prediction of the vacuum level change in vacuum insulation systems as a function of time. The program takes into consideration all the gas sources that cause deterioration at vacuum level and the effect of getter material [2]. VACSIM simulation program has two different applications for VIPs and VICs

2.4.1. VACSIM-VIP

Thermal performance of a vacuum panel is high, because heat transfer by conduction and convection are minimized by evacuation process and radiation is neglected. After evacuation process, it is very difficult to keep vacuum level in the panel at a constant. Permeability of barrier material and outgassing of inner filler material play an important role on pressure increase in the panel, that causes vacuum level change. Therefore the effect of these materials should be defined before designing a vacuum panel.

VACSIM-VIP program was developed to predict vacuum level change inside the panel with respect to time. It based on four main factors; barrier material, inner filler material, getter material and flange region of barrier material. In Figure 2.6 the main page of VACSIM-VIP simulation program is given. VACSIM-VIP program is important to develop new barrier materials and new inner filler materials for insulation, and it is also able to evaluate getter system in vacuum panel. By using this program, mostly effective VIP design can be determined and the lifetime of VIP can be predicted [10].

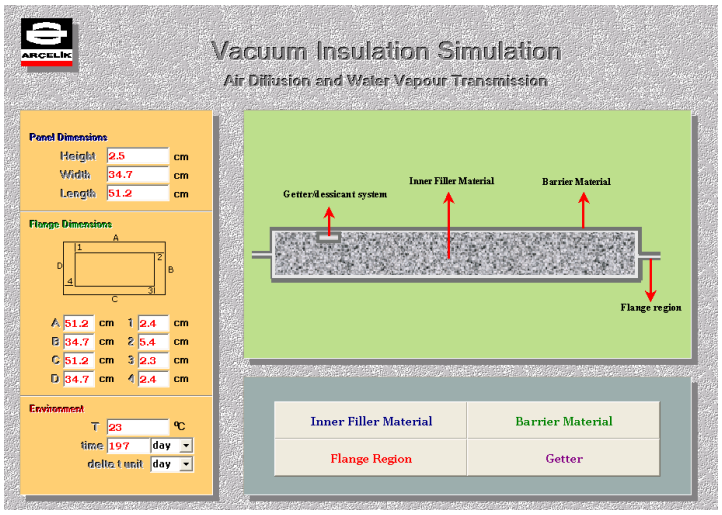

Figure 2.6: VACSIM –VIP main page

VACSIM calculations based on pressure change as a function of time as given in equation 2.9.

$$V\frac{dP_i}{dt} = \left(k_{i,s} + k_{i,f}\right)\left(P_{i,e} - P_i\right) + C_i t^{-\alpha_i} + B_i t^{-\beta_i} \qquad (2.9)$$

Left side of equation represents the change in partial pressure rate of gas "i", where the right side represents partial pressures related to diffusion from the surface and flanges of barrier material and partial pressure increase due to outgassing of inner filler material and barrier material respectively. α and β values change between 0.5-1 according to the inner filler material. Pressure at time t can be calculated by equation 2.10, where $P_{i,e} >> P_i$ [6].

$$P_i(t) = P_{init,t} + \left[\left(k_{i,s} + k_{i,f}\right)P_{i,e}t + \int C_i t^{-\alpha} dt + \int B_i t^{-\beta_i} dt\right] \div V \qquad (2.10)$$

For last two terms in equation 2.10, integration begins from t=1. If α and β values are less than 1, equation 2.11 is used instead of equation 2.10. But if α and β values are equal to 1, equation 2.12 should be used.

$$P(t) = \sum_1^N P_{init,i} + \left[t\sum_1^N P_{e,i}\left(k_{i,s} + k_{i,f}\right) + \sum_1^N \left(\frac{C_i}{1-\alpha_i}\right) t^{(1-\alpha_i)} + \sum_1^N \left(\frac{B_i}{1-\beta_i}\right) t^{(1-\beta_i)}\right] \div V \qquad (2.11)$$

$$P(t) = \sum_1^N P_{init,i} + \left[t\sum_1^N P_{e,i}\left(k_{i,s} + k_{i,f}\right) + \sum_1^N C_i \ln t + \sum_1^N B_i \ln t\right] \div V \qquad (2.12)$$

In order to keep vacuum level constant, a getter system has to be used in a vacuum insulation system. The effect of getter material maintains until it fulfils its capacity. A

getter system with capacity G (pressure x volume) can decrease the pressure increase in a vacuum panel, as the division of capacity of getter to volume of the panel (V). If the effect of getter system is fit in equation 2.11, it will be equation 2.13, when α and β values are less than 1.

$$P_i(t) = P_{init,t} + \left[P_{e,i}\left(k_{i,s} + k_{i,f}\right)t + \left(\frac{C_i}{1-\alpha_i}\right)t^{(1-\alpha_i)} + \left(\frac{B_i}{1-\beta_i}\right)t^{(1-\beta_i)} \right] \div V - \frac{G_i}{V} \quad (2.13)$$

If α and β values are equal to 1, getter effect is fit into equation 2.16 and equation 2.18 is used in calculations [10].

$$P_i(t) = P_{init,t} + \left[P_{e,i}\left(k_{i,s} + k_{i,f}\right)t + C_i \ln t + B_i \ln t\right] \div V - \frac{G_i}{V} \quad (2.14)$$

If a vacuum panel includes getter system, equations 2.13 and 2.14 should be used instead of equation 2.11 and 2.12.

2.4.1.1. Barrier Material

According to Fick's law, total volume of gas (V) that is permeating through a barrier layer is directly proportional to the area (A) of the barrier layer, the partial pressure difference of the penetrant (Δp) between the two sides of the barrier. On the other hand, it is inversely proportional to the barrier layer thickness (d).

By a combination of these parameters, gas permeability can be calculated related to equation 2.15 [5].

$$P=V.s / (A.p.t) \quad (2.15)$$

Fick's first law is applicable only for gases such as air, oxygen, argon and carbon dioxide, which obey to Henry's law and proportionally relates the solubility of the penetrant in the barrier to the partial pressure of the penetrant. Fick's first law for vapors lke H_2O, which are liquid at pressure and temperatures close to normal, can be expressed by equation 2.16. Equation 2.16 can be used only for gases that liquefy under much lower pressures and temperatures than normal conditions (1 atm and 0 ^{0}C), like air, O_2, N_2, Ar and CO [5].

$$VTR= W.s / (A.t) \quad (2.16)$$

In the case of a barrier layer composed of different types of plastic films, the gas permeability coefficient of the multilayer plastic system is given in Equation 2.17,

where n represents the number of the different type of layers and d_i and P_i are the thickness and the gas permeability coefficient of each layer respectively [5].

$$P(cm^3/m^2.day,bar) = \frac{1}{\sum_i \frac{d_i(\mu m)}{P_i(cm^3.\mu m/m^2.day.bar)}} \tag{2.17}$$

In the case of a multilayer plastic system, the total water vapor transmission rate is expected to follow the relation given by equation 2.18.

$$WVTR = \frac{1}{\sum_{i=1}^{n} \frac{d_i}{WVTR_i}} \tag{2.18}$$

VACSIM program calculates the permeability by considering both cases of permeation: i) Through the whole surface of the barrier material, related page is shown in Figure 2.7 ii) Through the flanges of the enclosed evacuated vacuum system related page is given in Figure 2.8.

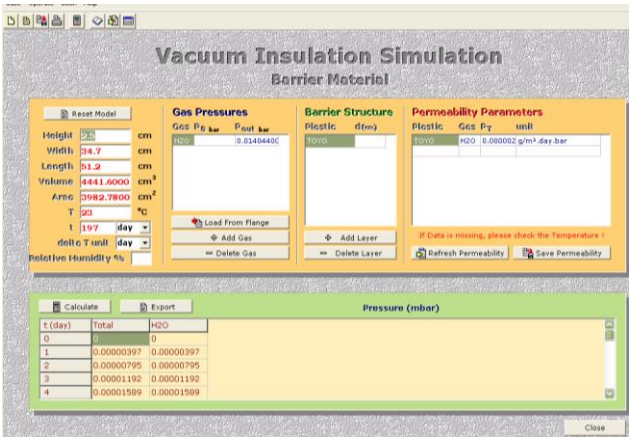

Figure 2.7: VACSIM-VIP 'Barrier Material' page

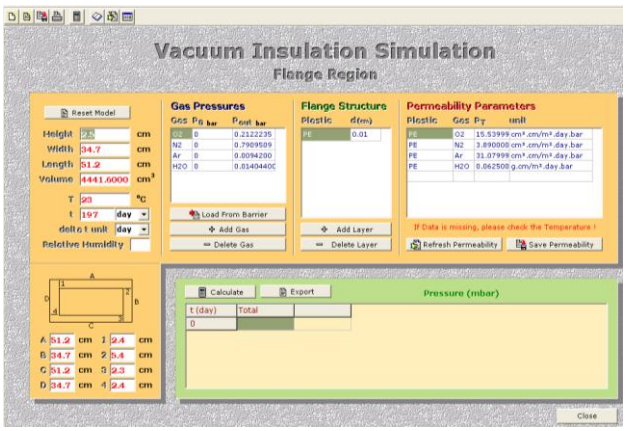

Figure 2.8: VACSIM-VIP, 'Flange Region' page

2.4.1.2. Getter Material

Getter materials are used to prevent pressure increase in the panel as it was discussed in section 2.3.5. VACSIM calculates the amount of accumulated gas in the panel caused by permeation through barrier material and outgassing from inner filler material in specified time duration. This calculation is made for each of the atmospheric gases separately. The capacity of getter material is then compared to the amount of the accumulated gas. And getter system is evaluated by two aspects:

- It controls, if selected getter system is sufficient to absorb total amount of gas accumulated in panel or not. If the answer is yes, it gives a result as “Acceptable”. If program gives the result as “Not-accepted”, then the getter system can be changed; the amount of getter material can be increased; the geometry or other components of vacuum panel may be changed.
- It controls, if pressure increase in panel reaches to critical pressure of inner filler material during the lifetime of VIP or not. If it does not reach, then the system is available for usage in VIP, but if it reaches to critical pressure then the system should be improved.

VACSIM-VIP getter page is shown in Figure 2.9. Getter menu was provided to analyze panel systems both with or without getter material. Figure 2.10 shows the no getter option to evaluate the panel.

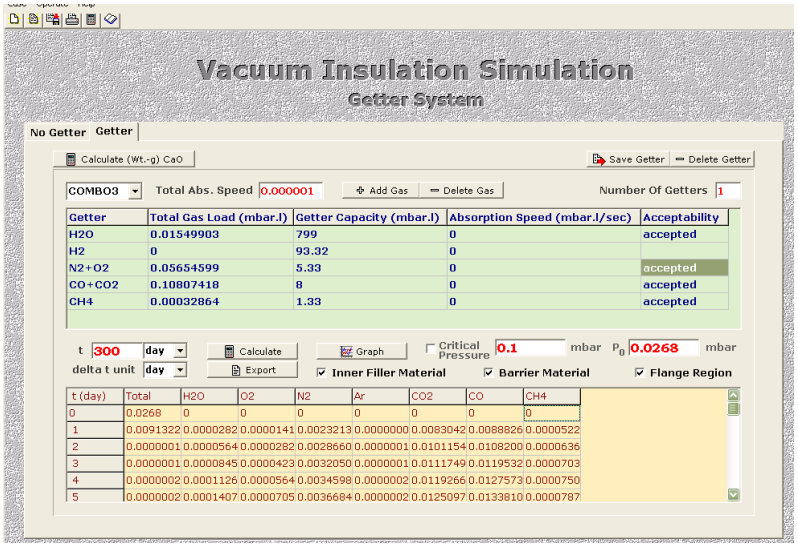

Figure 2.9: VACSIM-VIP; Getter System page

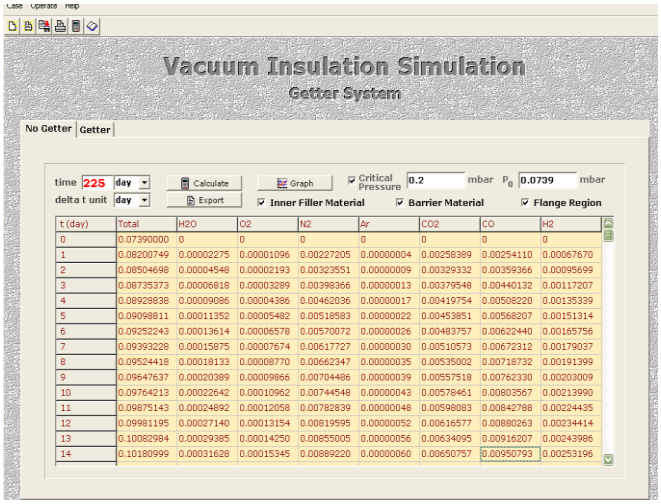

t (day)	Total	H2O	O2	N2	Ar	CO2	CO	H2
0	0.07390000	0	0	0	0	0	0	0
1	0.08200749	0.00002275	0.00001096	0.00227205	0.00000004	0.00258389	0.00254110	0.00067670
2	0.08504698	0.00004548	0.00002193	0.00323551	0.00000009	0.00329332	0.00359366	0.00095699
3	0.08735373	0.00006818	0.00003289	0.00398366	0.00000013	0.00379548	0.00440132	0.00117207
4	0.08928838	0.00009086	0.00004386	0.00462036	0.00000017	0.00419754	0.00508220	0.00135339
5	0.09098811	0.00011352	0.00005482	0.00518583	0.00000022	0.00453851	0.00568207	0.00151314
6	0.09252243	0.00013614	0.00006578	0.00570072	0.00000026	0.00483757	0.00622440	0.00165756
7	0.09393228	0.00015875	0.00007674	0.00617727	0.00000030	0.00510573	0.00672312	0.00179037
8	0.09524418	0.00018133	0.00008770	0.00662347	0.00000035	0.00535002	0.00718732	0.00191399
9	0.09647637	0.00020389	0.00009866	0.00704486	0.00000039	0.00557518	0.00762330	0.00203009
10	0.09764213	0.00022642	0.00010962	0.00744548	0.00000043	0.00578461	0.00803567	0.00213990
11	0.09875143	0.00024892	0.00012058	0.00782839	0.00000048	0.00598083	0.00842788	0.00224435
12	0.09981195	0.00027140	0.00013154	0.00819595	0.00000052	0.00616577	0.00880263	0.00234414
13	0.10082984	0.00029385	0.00014250	0.00855005	0.00000056	0.00634095	0.00916207	0.00243986
14	0.10180999	0.00031628	0.00015345	0.00889220	0.00000060	0.00650757	0.00950793	0.00253196

Figure 2.10: VACSIM-VIP, “No Getter” option

VACSIM also calculates the needed amount of CaO in getter material, which is responsible of absorbing water vapour (Eq 2.19). Calculation page for this option is shown in Figure 2.11.

$$M=\Delta P*V*0.00005784*18*t*5 \qquad (2.19)$$

M =needed amount of CaO (g)

ΔP= pressure increase in the panel per unit time (torr)

V =volume of panel (l)

0.00005784 Mw = 1 torr

Mw=18 g/mol (for water)

t= life time of panel (year)

5= safety factor

18= weight of 1 mol water vapour (g)

Figure 2.11: VACSIM-VIP, Calculation page for the amount of CaO

In getter menu, if critical pressure of inner filler material was added into “Critical Pressure” part, program is able to give a graph, that shows if pressure increase inside the panel reaches to critical pressure value or not. An example of such a graph is given in Figure 2.12.

Figure 2.12: VACSIM-VIP-No getter/Graph page

2.4.1.3. Outgassing from Inner Filler Material

The generation of gas resulting from the desorption is known as outgassing and it can be expressed in terms of the outgassing constant. The outgassing values of the inner filler materials can be fitted by using an empirical equation (Eq.2.20), where g(t) and g_0 are the outgassing rates at a specific time (t) and at one-hour time respectively, where t is the time in hours. α is the parameter that changes between 0.5-1 due to outgassing mechanism of material. When equation 2.20 is integrated over time, the pressure contribution coming from the outgassing of the inner filler material can be calculated at a specific time [8]. VACSIM- Inner filler material page is shown in Figure 2.13.

$$g(t) = g_0 (t)^{-\alpha} \tag{2.20}$$

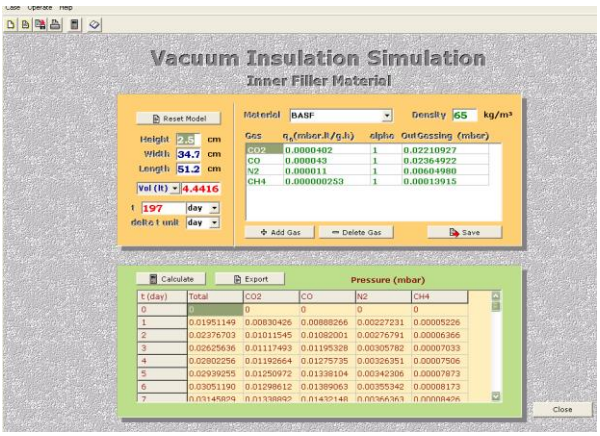

Figure 2.13: VACSIM-VIP; 'Inner Filler Material' page

2.4.2. VACSIM-VIC

VACSIM-VIC simulation program was provided to predict vacuum level change in a VIC with respect to time. It is based on three main factors, which are permeability, outgassing and getter material. In Figure 2.14 the main page of VACSIM-VIC is

given. In this thesis, only permeability effect is taken in consideration for VIC concept.

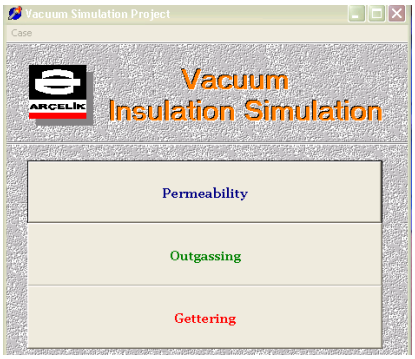

Figure 2.14: VACSIM-VIC Main Page

VACSIM-VIC calculates pressure increase in the insulation volume, caused by permeation through barrier material, in two sections as water vapour permeation and gas permeation. It gives the result as an addition of these two section results. To make a simulation by VACSIM-VIC program, barrier material thickness and environmental conditions should be introduced to the system, because permeability parameters are changeable with thickness of layer and environmental conditions like temperature and relative humidity. Permeability of plastic is proportional with temperature and relative humidity, where it is inverse proportional with thickness of barrier material. VACSIM-VIC program can be used to determine the most effective barrier structure with optimum thicknesses [19].

2.4.2.1. Effect of Gas Permeation on Pressure Increase

In a VIC cabinet, gas pressures at the inside of the cabinet, at outside condition and in insulation volume are different from each other. Gas diffusion occurs from high gas pressure side to low gas pressure side between these three environments. It is assumed that insulation volume is fully evacuated and pressure is zero at the beginning. That is why gas diffusion occurs from the inner and outer parts of cabinet to the insulation volume, as it is shown in Figure 2.15 [4].

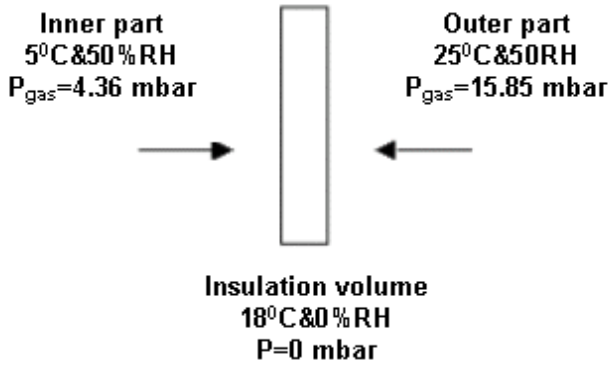

Figure 2.15: Gas diffusion from inner and outer parts of cabinet to insulation volume due to pressure difference

2.4.2.2. Gas Permeation Through Monolayer Structures

Pressure increase in evacuated insulation volume of the VIC is calculated firstly by determining the volume of accumulated gas in the cabinet and then converting the result into the pressure. The volume of gas is calculated according to the equation 2.21, as it was described in section 2.1.1.

$$V = \frac{p(A * \Delta P * t)}{d} \tag{2.21}$$

Permeability of plastic barrier materials changes with respect to temperature. That is why permeation from the inner part and outer part of cabinet should be calculated separately and then added to find total volume of gas in evacuated insulation volume, as it is shown in equation 2.22 [11]. V_{gas} is the total volume permeated in insulation volume; V_{in} is the gas volume that diffused from inner part of cabinet into insulation volume and V_{out} is the gas volume diffused from outer part of cabinet into insulation volume.

$$V_{gas}=V_{in}+V_{out} \tag{2.22}$$

If insulation volume was not evacuated, it would filled with air and the pressure in insulation volume would be equal to atmospheric pressure that is 1013 mbar. The iteration is provided as below, where V_{gas} is the total volume of penetrating gas, V is the insulation volume and ΣP_1 is the pressure increase at the end of first unit time.

$$\Delta P=P_{atm}-\Sigma P_{in} \tag{2.23}$$

$$\Delta P_0=P_{atm}-\Sigma P_0 \quad (\Sigma P_0 =0 \text{ mbar}) \tag{2.24}$$

$$\Sigma P_1 = \frac{P_{atm} * V_1}{V} \quad (2.25)$$

$$\Delta P_1 = P_{atm} - \Sigma P_1 \quad (2.26)$$

$$P_2 = \frac{\Sigma P_1 * \Delta P_1}{\Delta P_0} \quad (2.27)$$

$$\Sigma P_2 = \Sigma P_1 + \Sigma P_2 \quad (2.28)$$

$$\Sigma P_3 = \Sigma P_2 + \frac{\Sigma P_1 * \Delta P_2}{\Delta P_0} \quad (2.29)$$

.

.

.

$$\Sigma P_{n+1} = \Sigma P_n + \frac{\Sigma P_1 * \Delta P_0}{\Delta P_0} \quad (2.30)$$

P represents, pressure increase on insulation volume at the end of unit time. In general, pressure increase in evacuated volume is calculated due to equation 2.31. This calculation is carried on by iteration until to reach desired time duration as described above. The main page of VACSIM-VIC permeability part is given in Figure 2.16.

$$\Delta p_1 = \frac{\Delta p_0 * 10^{-3} * \Delta t * \left(\frac{P_{in} * A_{in} + P_{out} * A_{out}}{d} \right) * P_{out}}{V} \quad (2.31)$$

$\Delta p_0 = P_{out} - P_{in}$= 1013 mbar- 0 mbar = 1013 mbar (Converted to bar by multiply 10^{-3})

P_{out} = 1.013 bar (Pressure value of outside conditions)

P_{in} = 0 bar (Pressure value of insulation volume after evacuation process)

Δt = time duration(1 day)

A_{out}= Outside area of plastic barrier material (m^2)

A_{in} = Inside area of plastic barrier material (m^2)

P_{out} = Permeability of barrier material at outside temperature conditions (cm^3*cm/ m^2*day*bar)

P_{in} = Permeability of barrier material at inside temperature conditions (cm^3*cm/ m^2*day*bar)

d= Thickness of barrier material (cm)

V= Volume of evacuated insulated part (cm^3)

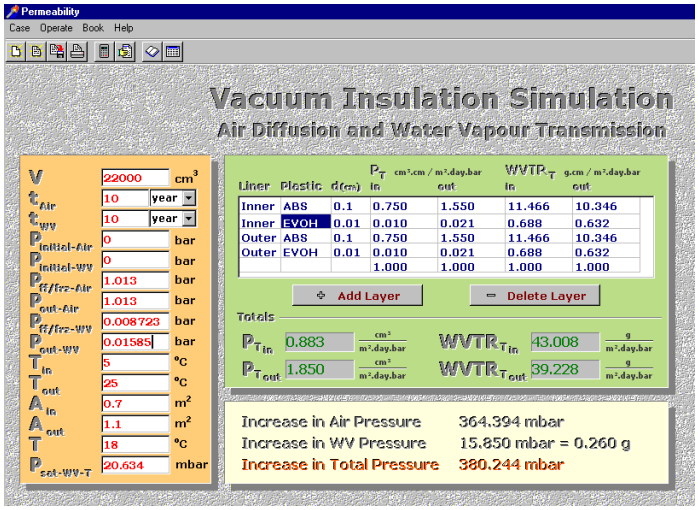

Figure 2.16: VACSIM-VIC; Main Menu for Permeability Section

2.4.2.3. Gas Permeability Through Multilayer Structures

In the case of a barrier material composed of different types of plastic layers, the gas permeability coefficient of the multilayer plastic is given by equation 2.32. It has the same logic that was discussed in section 2.4.1.1 [11].

$$P = \frac{1}{\sum \frac{d_i}{P_i}} \tag{2.32}$$

$P\left(\frac{cm^3}{m^2.day.bar}\right)$ = Total permeability of multilayer structure

d_i (cm)=Thickness of each layer

$P_i\left(\frac{cm^3.cm}{m^2.day.bar}\right)$ = Gas permeability of each layer

2.4.2.4. Effect of Water Vapor Permeation on Pressure Increase

One of the effects on pressure increase in evacuated volume is the water vapor permeation through barrier material. Environmental conditions for the insulation volume, for outside and inside of the cabinet are different from each other with respect to temperature and relative humidity. Due to this difference water vapor diffusion occurs from high pressure side to low pressure side. At the beginning, inside of the cabinet has higher vapor pressure than the pressure in insulation volume. Therefore diffusion occurs from the inner side to the insulation volume. By the same logic, the pressure at the outside of the cabinet is higher than the pressure in insulation volume and again diffusion occurs from outside to the insulation volume.

Relative humidity of environmental conditions and the temperature are the most important factors in calculation of pressure increase caused by water vapor permeation through plastic. If relative humidity increases, the amount of vapor permeates into insulation volume increases and the pressure also increases. Temperature is also important by calculation of permeation, the permeability increases as the temperature increases. Diffusion from the inside of cabinet to the insulation volume continues until the pressure in insulation volume reaches to the pressure of inner part at 100% relative humidity conditions. After this equilibrium state, pressure in insulation volume will be higher than the pressure in inside of the cabinet, because water vapor diffusion maintains from outside into insulation volume. At this point, the way of diffusion changes from insulation volume into the inner side of cabinet, as it is shown in Figure 2.18. Temperature at inner part is lower than insulation volume and as a result diffusion rate is very slow, because permeation decreases as temperature decreases [11].

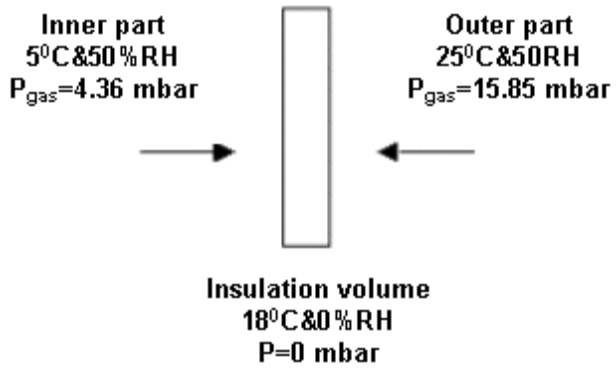

Figure 2.17: The way of diffusion, when water vapor pressure in insulation volume is zero.

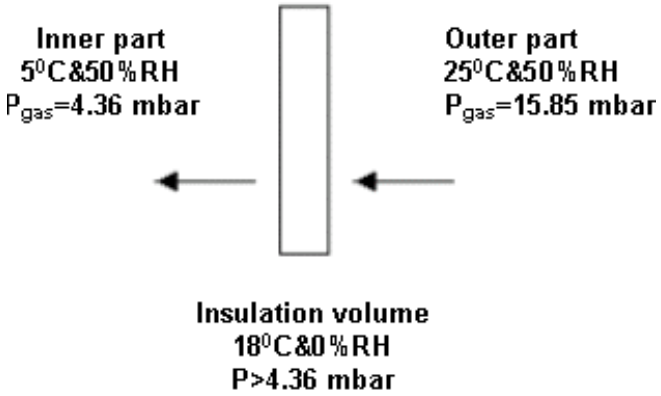

Figure 2.18: The way of diffusion, when water vapor pressure in insulation volume is higher than the pressure in inner part.

If the water vapor pressure on inner part of cabinet is higher than the pressure on insulation volume at 100% RH and insulation temperature, the diffusion occurs

always from inside and outside of the cabinet into the insulation volume. This continues until the pressure on insulation volume reaches to the pressure value that is at 100 % RH and insulation temperature. After that point, water vapor cannot create pressure increase and water vapor condensation begins. The steps of this phenomena is described below:

- Some amount of water vapor diffused in insulation volume is adsorbed by inner filler material until to reach its water absorption capacity.
- Water vapor diffuses into insulation volume and causes pressure increase. This pressure increase maintains until to reach the pressure at 100%RH conditions.
- More water vapor on insulation volume cannot cause pressure increase, but diffusion also continues from outside into the insulation volume. Water vapor begins to condensation.
- After the beginning of condensation, pressure on insulation volume remains as constant, which is known as saturation pressure. More amount of water vapor causes increase in weight of inner filler material.

By diffusion process ΔP changes continuously, that is why calculations have to be iterated with respect to time. Unit time for these calculations is selected as minute because relative humidity level reaches quickly to 100% in insulation volume [12].

Calculations for water vapor permeation are based on Fick's first law that is similar to gas permeation as explained in section 2.3.2. First of all the amount of permeating water vapor is calculated and then it is converted into pressure units as given in equations 2.33-2.38 [11].

$$W_{H_2O} = \frac{WVTR * A * \Delta t}{d} \tag{2.33}$$

W_{H2O} (g)= The amount of water vapor collected in insulation volume

$WVTR\left(\frac{g.cm}{m^2.day.bar}\right)$=Permeability of plastic

A (m^2)= Surface area

d (cm)= Thickness of barrier material

Δt (day)= Time

$$W_{H_2O} = W_{T_{in}} + W_{T_{out}} \tag{2.34}$$

$W_{T(in)}\ \left(\frac{g.cm}{m^2.min}\right)$= Amount of water vapor diffused from inner side of cabinet into insulation volume

$W_{T(out)}\ \left(\frac{g.cm}{m^2.min}\right)$= Amount of water vapor diffused from outer side of cabinet into insulation volume

After total amount of water has been calculated, it is converted into pressure units.

$$W = \frac{\Delta t * (W_{in} * A_{in} + W_{out} * A_{out})}{d} \quad (2.35)$$

$$PV = nRT \quad (2.36)$$

$$PV = \frac{W}{18}RT \quad (2.37)$$

P (mbar)= Pressure

n (g/mol)= Mol number (1 mol H_2O=18 g/mol)

R (lt.atm/mol.K)= Ideal gas constant

T (^{0}C)= Temperature

V (lt)= Insulation volume

This calculation is iterated until desired measurement time, as in section 2.3.1. The conditions at outside the cabinet are assumed as 25^{0}C&50% RH and water vapor pressure is 15.85 mbar, thus the pressure difference between insulation volume and outer part is 15.83 mbar after evacuation process, when water vapor pressure is zero. First pressure difference between outside pressure and inside pressure is 15.85 mbar, after permeation of water vapor pressure increase is p_1. To make further calculations for pressure increase, new pressure difference should be determined. General formula for determining pressure increase can be given as in equation 2.38 [11].

$$P_n = P_{n-1} + \frac{P_{out} - P_{n-1}}{P_{out}} * p_1 \quad (2.38)$$

P_n= Pressure level at the end of time n.

P_{n-1}= Pressure level at the end of time n-1

P_{out}= Water vapor pressure of outside conditions

p_1= First pressure increase after evacuation process

2.4.2.5. Water Vapor Permeability Through Monolayer and Multilayer Structures

To find total pressure increase caused by water vapor permeation, firstly the amount of permeated gas is calculated and then it is converted into pressures. For monolayer structures the permeability value of the layer is used in calculations, where for multilayer structures water vapor permeability value is calculated for each of the layers one by one and then they are added to have a single permeability value, as in equation 2.39 [11].

$$WVTR = \frac{1}{\sum_i \frac{d_i}{WVTR_i}} \tag{2.39}$$

$WVTR\left(\frac{g.cm}{m^2.day}\right)$ = Water vapor permeability of multilayer structure

$WVTR_i\left(\frac{g.cm}{m^2.day}\right)$ = Water vapor permeability of monolayer structure

d (cm)= Thickness of plastic layer

2.4.2.6. Total Permeability Effect

The pressure of evacuated insulation volume, increases as a result of gas and water vapor permeation with respect to time. This pressure increase should be determined definitely to obtain when it reaches to critical pressure of inner filler material. These determinations help to select best monolayer structure or multilayer structure.

Total permeability effect is calculated by adding pressure increases caused by gas and water vapor permeation, as in equation 2.40 [11].

At the end of 1^{st} unit time $P_1=P_1$ (gas pressure)+ P_1 (water vapor pressure)

At the end of 2^{nd} unit time $P_2= P_2$ (gas pressure)+ P_2 (water vapor pressure)

At the end of n^{th} unit time $P_n= P_n$ (gas pressure)+ P_n (water vapor pressure) (2.40)

VACSIM program gives three different results these are “Increase in air pressure”, “Increase in WV pressure” and “ Increase in total pressure”. Pressure increase related to gas permeation is given in “Increase in air pressure” section with mbar unit. Pressure increase related to water vapor permeation is given in “Increase in WV pressure” in mbar and gram units. The addition of these two results is given in “Increase in total pressure”.

VACSIM calculates permeability of a plastic at any temperature due to Arrhenius equation (Eq.2.41). To find the permeability value for a desired temperature, at least two different permeability values of selected plastic should be introduced to the system.

$$P = P_0 e^{-\frac{E_a}{RT}} \tag{2.41}$$

$$\ln(P) = \ln(P_0) - \frac{E_a}{RT(^0K)} \tag{2.42}$$

$P(cm^3.cm/m^2.day.bar)$=Permeability value of plastic material at T (^0K)

$P_0(cm^3.cm/m^2.day.bar)$=Permeability value of plastic material where $T \longrightarrow \infty$

E_a(atm.l/mol)=Activation energy

R(0.082 atm.l /mol.K)=Ideal gas constant

T(^0K)=Temperature

If two different permeability values for a plastic are known, $\ln(P_0)$ and (E_a/R) values could be find by using equation 2.43 and 2.44.

$$\ln(P_1) = \ln(P_0) - \frac{E_a}{RT_1} \tag{2.43}$$

$$\ln(P_2) = \ln(P_0) - \frac{E_a}{RT_2} \tag{2.44}$$

VACSIM calculates $\ln(P_0)$ and (E_a/R) values and saves the results. Thus at any temperature, permeability value of selected plastic can be found. The calculation menu of program is given in Figure 2.19.

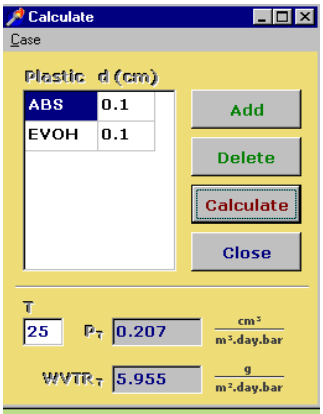

Figure 2.19: VACSIM-VIC; Archieve Menu/“Calculate” option

“Water Pressure Table” section of VACSIM program provides to see water vapor pressure values at any temperature between –15^{0}C-100^{0}C and 100% relative humidity conditions. The values are presented as both mbar and mmHg units.

Pressure increase from the beginning until the end of desired time duration can be determined in “Show Result” option. This section gives the result as a table such in Figure 2.20.

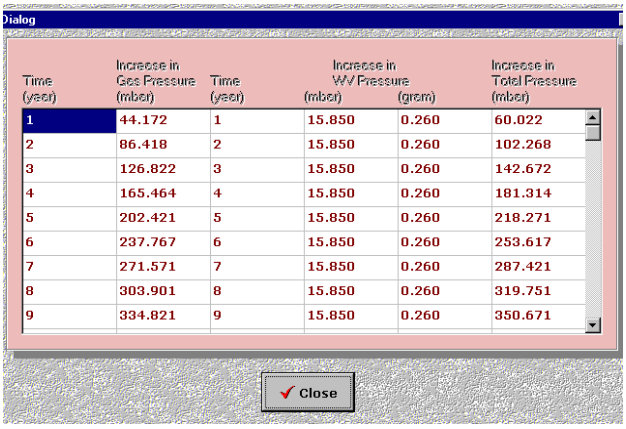

Figure 2.20: VACSIM-VIC; “Show results” page

3. EXPERIMENTAL

3.1. Material

3.1.1. Barrier Material

Barrier materials used in VIP's are multilayer structures that have very low permeability values. Two different kinds of barrier films were researched among this thesis. The structures of films are described below:

- Film A: PA 15 μm/ metallized PET 12 μm/ Al 6 μm/ PE 40 μm
- Film B: PA (15 μm)/ metallized PET (12 μm)/ Al (5 μm)/ PE (40 μm)

The reasons of the usage for the structures are given below [13]:

- PA is used because of its high impact resistance; low gas permeability; easy to process; high tear strength and high tensile strength properties.
- PET is used for mechanical strength; thermal stability; low water vapor and gas permeation and high impact resistance.
- Al is used to prevent gas and water vapor permeation; to resist chemicals and to prevent heat transfer by radiation.
- PE is used for its properties such as easy to welding; low water vapor permeation; excellent chemical resistance and toughness at low temperatures.

3.1.2. Getter Material

Getter material, that is shown in Figure 3.1, consists of three different chemicals, $BaLi_4$, Co_3O_4 and CaO. To prevent a premature consumption of barium-lithium alloy with H_2O, the getter powder is covered with a substantial amount of a high efficiency drier calcium oxide (CaO), which chemisorbs moisture in the panel and leaves the $BaLi_4$ alloy the task of removing the most difficult gases like N_2. A third active material cobalt oxide (Co_3O_4) is used to get rid of H_2 and some of the most common blowing agents like cyclopentane, which can permeate into the panel during its life

time. These three active chemical powders are compressed in a stainless steel cover according to a configuration that offers optimum sorption performances and easy of usage. Getter material does not need any heating process for activation. It should be removed from its cover just before prior the production of VIP. After removing it from the cover, it should be placed in a few minutes into the panel to prevent completing the capacity [14, 21].

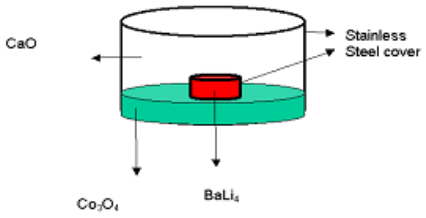

Figure 3.1: Schematic structure of getter material

In this study, gettering properties were investigated on three different types of getter materials. The ingredients of evaluated getters were same, but in different quantities. The comparisons of the ingredients are given in Table 3.1 [20].

Table 3.1: Evaluated getter materials

Getter Type	INGREDIENTS		
	CaO	Co_3O_4	$BaLi_4$
Getter A	**2.7 g**	**0.85 g**	**0.17 g**
Getter B	**2.7 g**	**0.45 g**	**0.09 g**
Getter C	**2.7 g**	**0.20 g**	**0.04 g**

The advantage of getter material in VIPs was also determined experimentally by measuring the pressure increase in two different types of VIPs with and without getter material. Inner filler materials of panels were open cell extruded polystyrene (XPS) and open celled polyurethane (OCPU), as they are shown in Table 3.2.

Table 3.2: Vacuum panels with/without getter material

A	**XPS-with getter (XPS-G)**
B	**XPS-without getter (XPS-NG)**
C	**OCPU-with getter (OCPU-G)**
D	**OCPU-without getter (OCPU-NG)**

3.2. Equipments

The measurement of absorption characteristics of getter materials and barrier permeability were carried out by high vacuum stainless steel test bench that was specially designed for Arçelik Research and Technology Development Center. The pictures of the test bench can be seen in Figure 3.2, Figure 3.3 and Figure 3.4. The equipments of the bench that are given below:

- Ionization gages (IG1, IG2): Bayerd-Albert type, Granville-Phillips Series 274
- Capacitance Manometer (CG1, CG2): MKS Baratron type 627, 626
- Rotary vane pumps (PM1, PM2, PM3): Pfeiffer Mode DUO 2.5
- Turbomolecular pumps (TP1, TP2): Pfeiffer Mod. TMU-065
- Mass spectrometer: Balzers QMA 200- Prisma (0-200 amu)
- Data collecting system: Balzers Quadstar MKS DL 4000

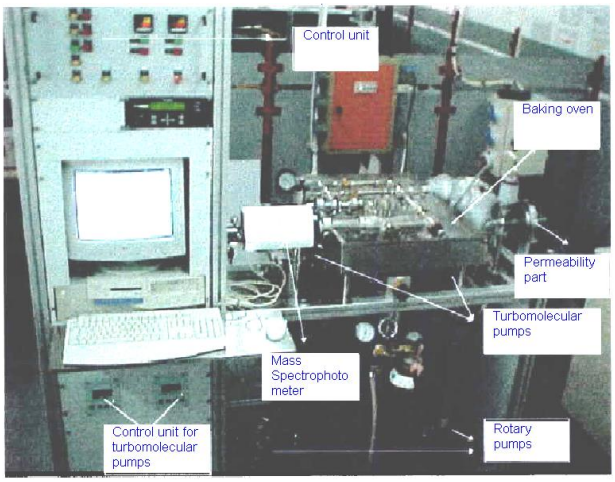

Figure 3.2: Stainless steel high vacuum test bench

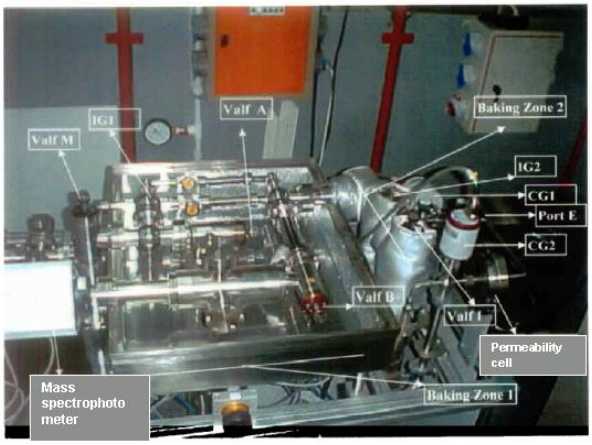

Figure 3.3: Detailed photograph of high vacuum stainless steel test bench

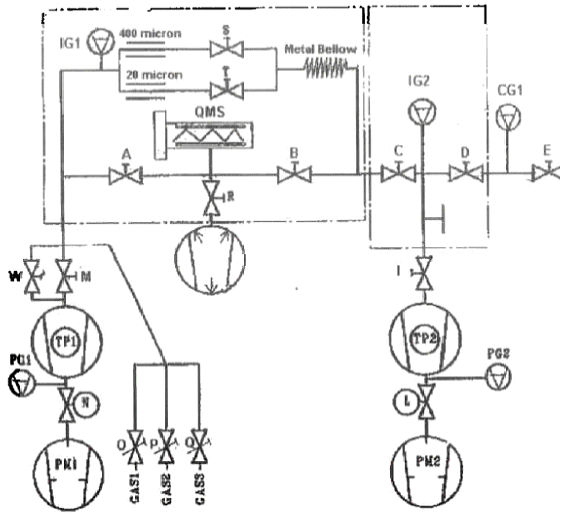

Figure 3.4: Scheme of the stainless steel high vacuum bench, equipped with the mass spectrometer for tests on vacuum components

3.2.1. High Vacuum Stainless Steel Test Bench

Permeability and gettering measurements were performed by stainless steel high vacuum test bench system. The bench consists of many tubes and connection parts. It contains two baking units for baking process, these are working with resistance heating. To open and close the selected volume part there are many valves on the system (A, B, C, D, E, F, G, H, I, L, M, N, O, P, Q, R, S, T, W). To achieve high vacuum, the bench contains two pumping groups, these are two turbomolecular pumps, TP1, TP2 and two rotary pumps, PM1, PM2. Rotary pumps are used for pre-vacuum that is about 10^{-3} torr. After pre-vacuum, turbomolecular pumps can be put into use and high vacuum levels can be achieved. If the system was open to the atmosphere, baking process should be applied to the system, before the usage of pumps. The necessity of baking process is to get rid of the water vapor that may sticked to the walls of the system. By using all the four vacuum pumps, the vacuum level can be reach at 10^{-10} torr levels. Pressures in defined area can be followed by ionization gages (IG1, IG2), capacitance manometer (CG1) and pirani gages (PG1, PG2). Ionization gages can measure the pressure between 10^{-3}-10^{-10} torr and they represent the result as the equivalent pressure for N_2. Capacitance manometer, CG1 measures the pressure between 10-10^{-3} torr. The measurement range for pirani gages are between rotary pumps and turbomolecular pumps, it measures the fore vacuum that is 760-10^{-3} torr. Pumping of first pumping group is controlled by two conductances, which are placed after S and T valves, and have 400 μ and 20 μ □radius respectively [15].□□

After A and B valves a mass spectrometer is placed on the system. Determining the gas level in the system and the sort of gases can evaluated by mass spectrometer.

A special software program achieves working of mass spectrometer and data collection that is Balzers Quadstar MKS 400.

3.2.1.1. Permeability Measurements

The barrier materials used in VIP's have very low permeability values against gas and water vapor that they cannot be measured by conventional measurement methods. To quantitatively evaluate gas permeation through high quality barriers a new technique is used, which is based on the measurement of the helium transmission rate.

For permeability measurements a diffusion cell is attached to the bench at valve E as it is shown in Figure 3.5 [16]. The sample is mounted between two flanges and helium pressure between 1-1000 mbar is applied on one side of the sample, the other side being in view of a quadrupole mass spectrometer. A set of calibrated conductances is placed between the mass spectrometer and the pumps for evacuation. So, helium flow (F) through the conductance is measured with the mass spectrometer according to the equation 3.21 and 3.2 [15].

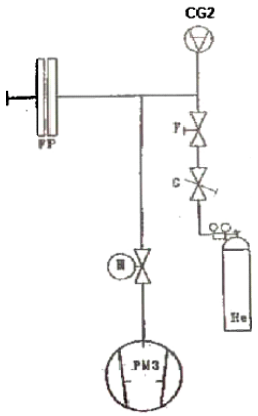

Figure 3.5: Schematic structure of the diffusion cell attached at E valve to the system

<u>Test method</u>

Gas flow related to applied pressure is given by F_1, the gas gone through the film and was pumped over conductances to QMS side is given by F_2 [12].

$$F_1 = k * P_{He}(\text{applied}) \quad (3.1)$$

$$F_2 = c_{He} * P_{He}(\text{QMS}) \quad (3.2)$$

Under equilibrium conditions, which can be reached after some minutes or some hours, depending on the sample, the gas flow F provide the helium permeation rate. At this condition, F_1 and F_2 will be equal to each other and permeability (k) value can be calculated as in equation 3.3.

$$k = \frac{c_{He} * P_{He}(QMS)}{P_{He}(applied) * A} \tag{3.3}$$

k=permeability, torr*l/s*torr

C_{He}=Conductance value for He, l/s

P_{He}(QMS)=Helium pressure at QMS side, torr

P_{He}(Applied)=Applied Helium pressure, torr

A=Diffusion area,m^2

The conductance values are different for each gas and they are changeable with respect to temperature and area of diffusion cell. In this thesis they are taken from literature [16].

3.2.1.2. Gettering Measurements

For gettering measurements a port is attached to the system that connect glass bulb, where getter material is placed. The picture of attached port is shown in Figure 3.6.

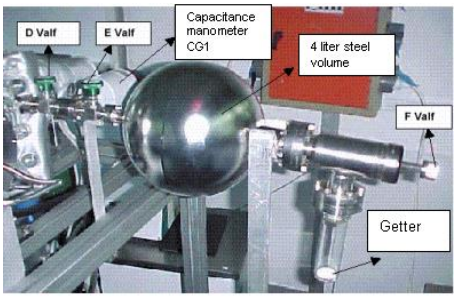

Figure 3.6: Attached part to the system for gettering measurements

Experimental conditions used in gettering measurements are:

System pressure: 10^{-8}, 10^{-9}

Getter material: Getter A

Applied pressure (test pressure): 1 torr

Isolated volume: 4469 cm^3 or 159 cm^3 (according to the adsorption characteristic of getter for selected gas)

Test method

Getter material was placed in glass bulb, and evacuated with all the system at the same time until vacuum level is reached to 10^{-8} mbar. After evacuation process the pumps for evacuation were closed and desired amount of test gas was sent on getter material. This amount is generally ~1torr of gas. The volume, where the test gas was collected and absorbed by getter was isolated from the system. Pressure decrease related to absorption was recorded due to time by a data collecting system.

Related to absorption by getter, pressure decreases. This maintains until the getter fulfills its absorption capacity. After the pressure decrease stopped, test was completed. Gettering speed (Q), and gettering capacity (C) for the test gas were calculated according to the equations 3.5 and 3.6.

$$Q = \Delta P * 1.33 * V_{isolated} * 1000 / \Delta t \quad (3.5)$$

$$C = \Delta P * 1.33 * V_{isolated} \quad (3.6)$$

3.3. Vacuum Level Measurements

Vacuum level measurements were achieved by using a device, called spirotorr vacuum gauge. The system consist of a sensor; a vacuum sensor head and a vacuum level indicator as it is shown in Figure 3.7. It is able to measure pressures between 10^{-3} –10^{3} mbar. VIP s should have vacuum level ranges between $5*10^{-2}$– 5 mbar. Thus, spirotorr vacuum gauges are able to determine the pressure increase inside the VIP' s as a function of time [19].

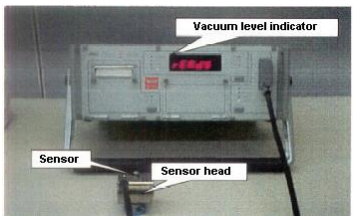

Figure 3.7: Spirotorr vacuum gauge

4. RESULTS AND DISCUSSION

In this thesis, the emphasis was given to determination of the getter material effect in vacuum level change for VIPs and multilayer structure effect in vacuum level change in VICs.

For VIP concepts the studies were focused on barrier permeability and gettering measurements. Permeability measurements were investigated in two different types of films. The results were compared with each other.

Gettering properties were investigated in three steps. In the first part, gettering characteristics for various gas types were determined experimentally. Selected test gas was sent on getter material and the pressure decrease was observed with respect to time. Gettering speed and gettering capacities were calculated for each of the tested gases. In the second part, three different types of getter materials were compared with each other related to their gettering properties. In the last part, vacuum levels in two different types of VIPs with and without getter material were measured with respect to time. This measurement was made by spirotorr vacuum gauge and it was also theoretically calculated by VACSIM simulation program. A comparison was made between experimental results and theoretical calculations.

For VIC concepts, multilayer plastic barrier structures were evaluated in three different systems. The determination of the best barrier structure with minimum permeability was achieved for first and second systems. The thickness optimization of the best structure was also achieved. All of the results were evaluated theoretically in VACSIM-VIC simulation program. The reliability of VACSIM–VIC was checked by comparing theoretical results to experimental results for third system.

4.1. Permeability Measurements for Film A and Film B

Permeability measurements were achieved for two different types of films, which were described in section 3.1.1. The measurements were followed respect to the method described in section 3.2.11.

Film A was measured firstly. Before measurement it was waited until He ion current reached an equilibrium state. The equilibrium state of ion current was observed by

mass spectrometer. When the pressure was recorded as 0 torr, firstly 23.6 torr gas was sent on film A and it was waited until ion current reaches the equilibrium again. At this equilibrium conditions ion current was measured as $1.13*10^{-13}$ mbar*l/ sec. To repeat the measurement 220.1 torr gas was sent on film and this time ion current reaches equilibrium at $4.39*10^{-13}$ mbar*l/ sec. Third gas was 755.8 torr and ion current was observed $1.56*10^{-12}$ mbar*l/ sec. It was observed that ion current level and applied pressures were in proportional. Observed ion current was converted into pressure as in equation 4.5.

$$k = \frac{3.92 * 10^{-2}\ \text{lt/sec} * (6.065\ \text{torr/amper} * (1.13 * 10^{-13} - 0)\ \text{amper})}{23.6\ \text{torr} * (2.36 * 10\ \text{cm}^{-2})} \quad (4.5)$$

$$k = 1.41*10^{-16}\ \text{torr*l/ torr*cm}^2\text{*sec} \quad (4.6)$$

Related to the gas pressures, permeability values were calculated as $k=1.64*10^{-16}$ torr*l/ torr*cm^2 sec and $k=1.97*10^{-16}$ torr*l/ torr*cm^2 sec. As a result mean permeability value of film A can be accepted as $1.67*10^{-16}$ torr*l/ torr*cm^2*sec.

Permeability of film B was calculated by same method. When ion current reached an equilibrium, 63.4 torr test gas was sent on film B. Ion current was measured as $2.58*10^{-11}$ mbar*l/ sec. To repeat measurement 155.8 torr gas was sent and this time ion current was observed as $3.02*10^{-11}$ mbar*l/ sec. Related to third repeat 357.8 torr gas was sent on film and ion current was measured as $3.63*10^{-11}$ mbar*l/ sec. Related to equation 4.7, permeability value of film B was calculated due to these three measurement.

$$k = \frac{3.92 * 10^{-2}\ \text{lt/sec} * (6.065\ \text{torr/amper} * (2.58 * 10^{-11} - 0)\ \text{amper})}{63.4\ \text{torr} * (2.36 * 10\ \text{cm}^{-2})} \quad (4.7)$$

$$k = 3{,}98*10^{-15}\ \text{torr*l/ torr*cm}^2\text{*sec} \quad (4.8)$$

Permeability values were calculated as $k=1{,}62*10^{-15}$ torr*l/ torr*cm^2 sec due to second test and $k=7{,}05*10^{-16}$ torr*l/ torr*cm^2 sec due to third test. As a result mean permeability value of film B can be accepted as $2.1*10^{-15}$ torr*l/ torr*cm^2*sec.

Permeability values of film A and film B were compared with each other. Film A was containing 1 μm less metal layer than film B. The permeability value of film A was calculated lower than the permeability of film B. This result supports that the thickness of metal layer is effective on permeability, if all the other layers in the structure are identical.

4.2. Gettering Measurements

4.2.1. Determination of Gettering Characteristics for Various Gas Types

Gettering characteristics of a getter type for atmospheric gases like N_2, CO, CO_2, O_2 and air were investigated by sending ~1 torr selected gas on getter material. Related to absorption of test gas, pressure decrease was observed with respect to time. It was waited until all of the sent gas was absorbed by getter and pressure decrease stopped. Then gettering speed and gettering capacities were determined.

4.2.1.1. Gettering Measurements for Nitrogen (N_2)

0.932 torr N_2 gas was sent on getter material. At the end of 10140 min. pressure value was observed 0 torr that means getter absorbed all the sent gas. The capacity value (C) was calculated 5.53 mbar*l due to equation 4.9, while gettering rate was determined from the graph in Figure 4.2 as $1.9*10^{-2}$mbar*cc/sec. As it is seen in Figure 4.1, gettering rate slows down with respect to time, however it seems constant at the beginning. The curve where it seems constant can be accepted as gettering rate.

$$C=0.932*1.33*4.469=5.53 \text{ mbar*} \quad (4.9)$$

$$Q = 0.932*1.33*4.469*1000/ \Delta t=1.9*10^{-2}\text{mbar*cc/sec} \quad (4.10)$$

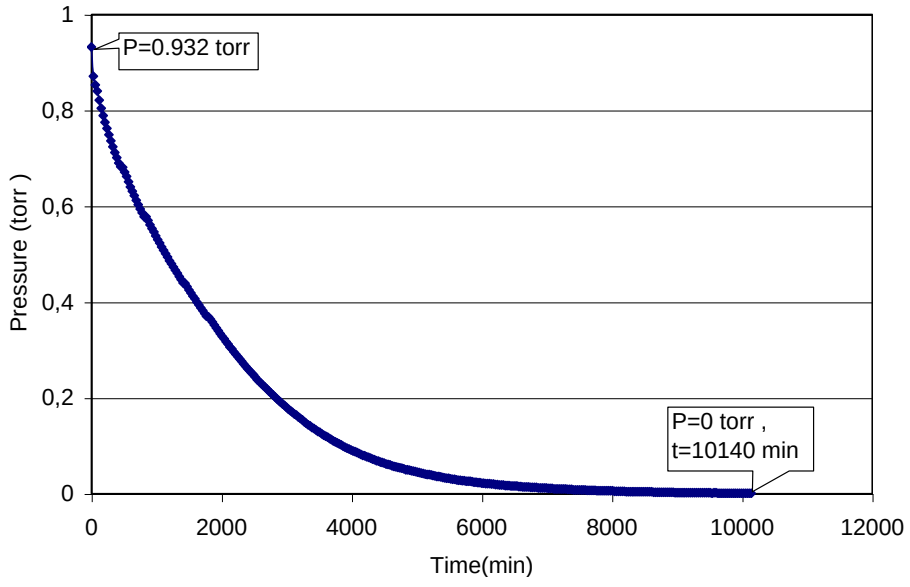

Figure 4.1: Pressure decrease observed in isolated volume due to N_2 gettering ($V_{isolated}$=4.469 liter)

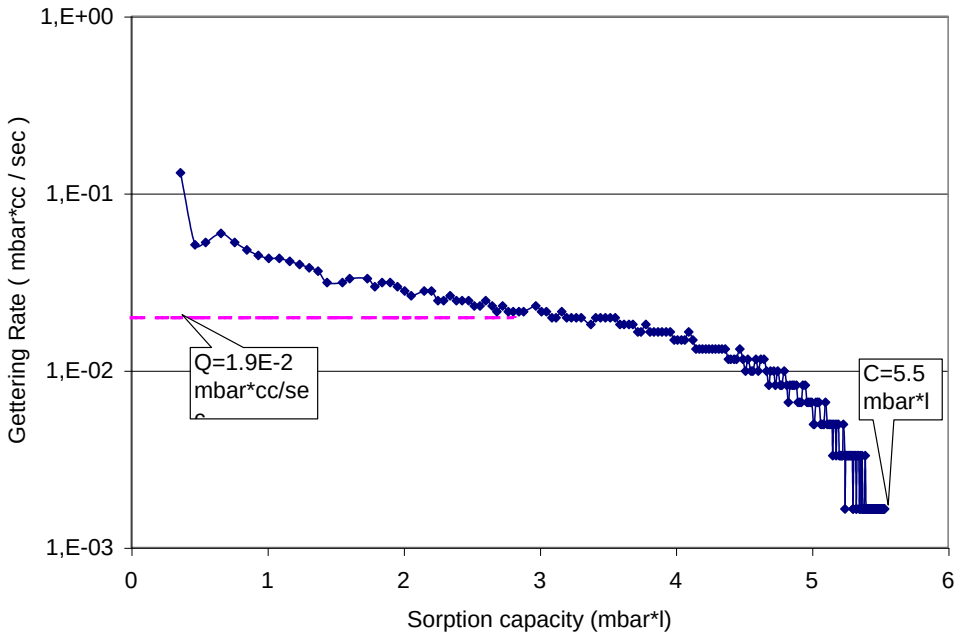

Figure 4.2: Gettering rate and sorption capacity of getter material for N_2 gas (P_{N2} = 0.932 torr, $V_{isolated}$= 4.469 liter)

4.2.1.2. Gettering Measurements for Carbon Monoxide (CO)

CO gettering measurements were achieved by sending 1.409 torr CO gas on getter material. Pressure decrease due to absorption maintained until 4054 minute. The curve related to this pressure decrease is given in Figure 4.3. Gettering capacity for CO was calculated 8.3 mbar*l as in equation 4.11, while gettering speed was determined 2.87 mbar*cc/sec as in Figure 4.4.

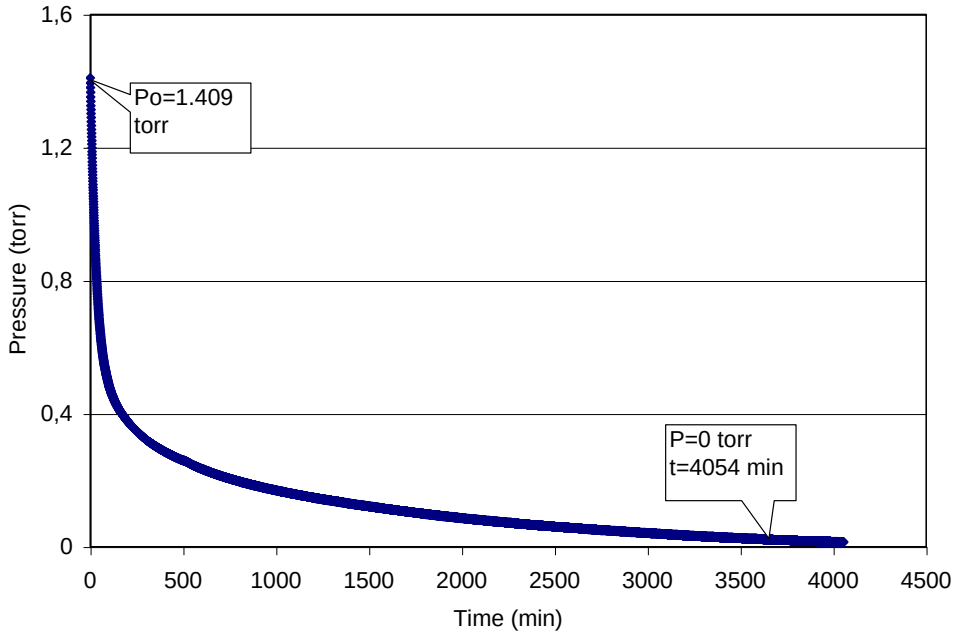

Figure 4.3: Pressure decrease observed in isolated volume due to CO gettering ($V_{isolated}$=4.469 liter)

$$C = 1.409 \square * 1.33 * 4.469 = 8.3 \text{ mbar*l} \quad (4.11)$$

$$Q = 1.409 * 1.33 * V_{isolated} * 1000 / \Delta t = 2.87 \text{ mbar*cc/l} \quad (4.12)$$

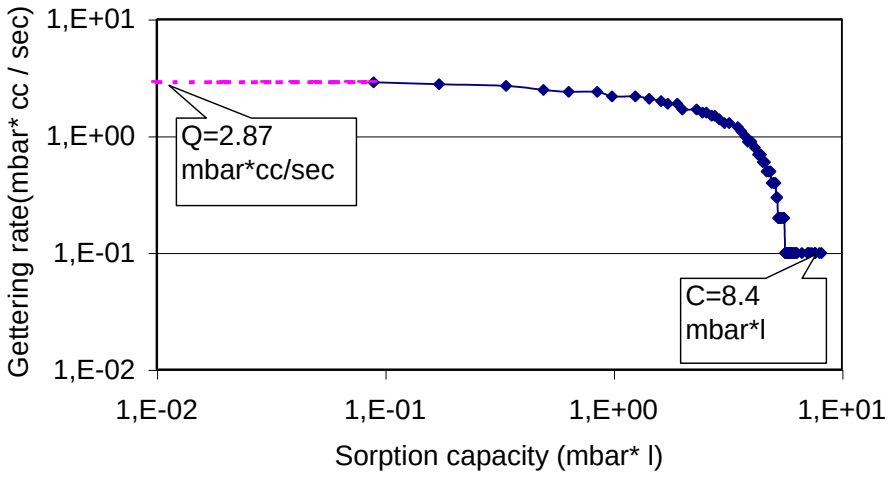

Figure 4.4: Gettering rate and sorption capacity of getter material for CO gas (P_{CO}=1.409 torr, $V_{isolated}$= 4.469 liter)

4.2.1.3. Gettering Measurements for Oxygen (O_2)

Around 1 torr gas O_2 gas was sent on getter material. Pressure decrease for O_2 was too slow to determine the gettering properties. Therefore O_2 gettering tests were repeated seven times by changing some factors that may effect gettering. In Figure 4.5 pressure decrease due to O_2 absorption and in Figure 4.6 gettering rate versus gettering capacity can be seen respectively.

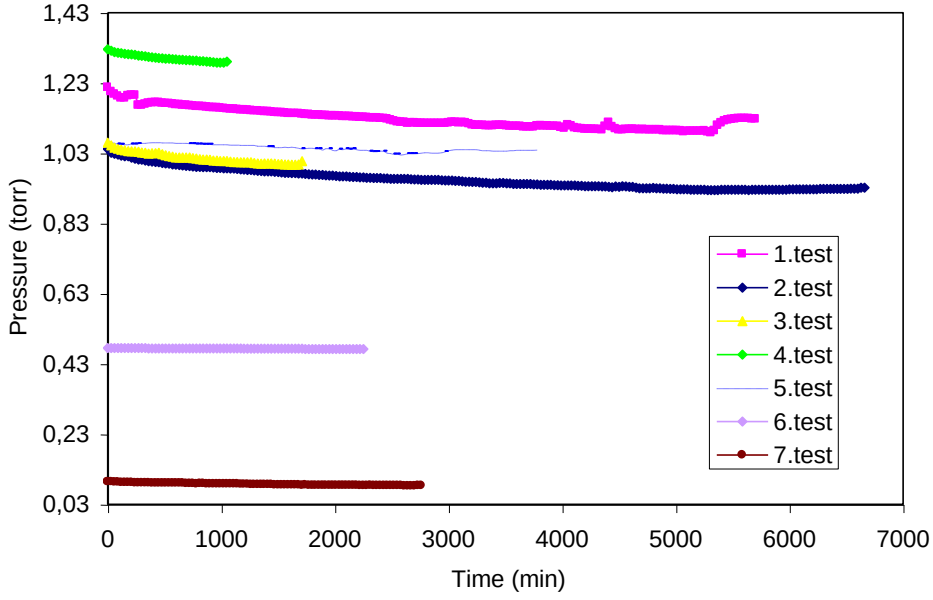

Figure 4.5: Pressure decrease observed in isolated volume due to O_2 gettering ($V_{isolated}$=4.469 liter)

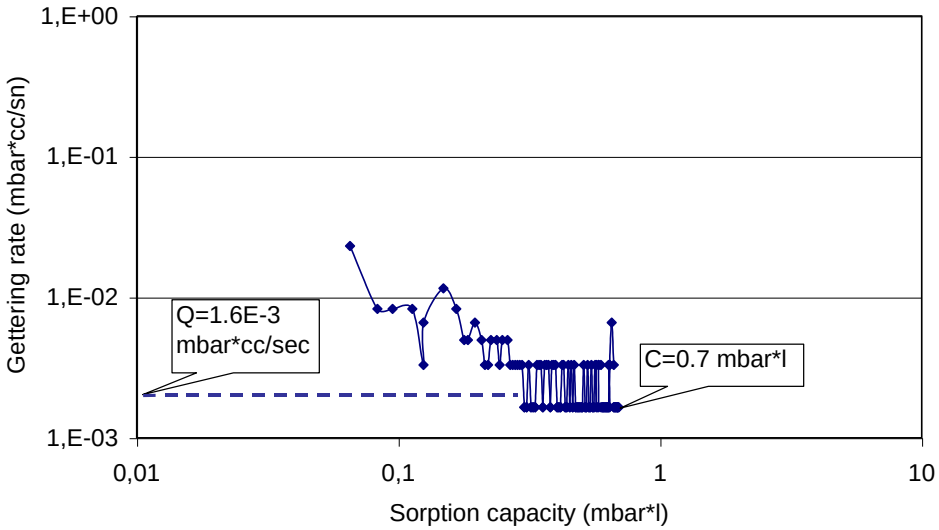

Figure 4.6: Gettering rate and sorption capacity of getter material for O_2 gas (P_{O2}=1.042 torr, $V_{isolated}$= 4.469 liter)

- First test was achieved by using big isolation volume. The amount of gas sent on getter material was P_0=1.217 torr. After 5310 minute observed pressure was P=1.088 torr. This pressure value was too low to determine the gettering rate and the capacity that is why test was repeated again.
- By making assumption that the observed pressure value in first test caused by some experimental defaults, the test was repeated without making any change on measurement system. 1.042 torr gas was sent on getter. After 6660 minute pressure was P=0.932 torr. According to this pressure difference gettering capacity was calculated 0.7 mbar*l, but gettering rate could not be determined.
- After second test, it was assumed that the getter may completed its capacity in time duration between removing it from the cover and to place into the test tube. Therefore third test was achieved by placing getter in the tube as quickly as possible. The amount of sent gas was P=1.06 torr and the pressure at the end of the test (1680 minute) was P= 0.988 torr.
- Fourth test was achieved by measuring new types of getter material by assuming that getter may completed its capacity in its cover. The pressure of sent gas was P_0=1.326 torr and the observed pressure was P=1.292 torr.

- After fourth test it was assumed that the problem may caused by O_2 gas. Therefore the gas in the O_2 tube was analyzed by mass spectrometer and it was proved that it is real oxygen. To be sure that the problem was not caused by capacity of getter, firstly N_2 was sent on it. N_2 adsorption occured successfully. This shows that the problem is not related to the getter material. N_2 test was stopped before getter completed its capacity and O_2 was sent on the same getter (P_{O2}=1.066 torr). But the same problem occurred, pressure decrease slowed down until P=1.039 torr and then stopped.
- For sixth test, the assumption was that, according to the Langmuir isoterm, sending less than 1 torr amount of pressure could be useful. So, P_0= 0.475 torr of O_2 was sent on getter, but the pressure decrease at the end of the test was only until P=0.472 torr.
- At 7.test, the amount of sent gas was reduced to P_0=0.094 torr, but the obtained pressure decrease was until P=0.083 torr.

O_2 tests that are described above, were achieved by using big isolation volume ($V_{isolated}$=4.469 liter). If big volume was used, the amount of sent gas will be around 4.469 torr*l on getter and this amount results in completing the capacity earlier than expected. Thus gettering rate and gettering capacity could not be calculated with respect to time. If the small isolation volume was used the amount of accumulated gas on getter material will be around 0.159 torr*l, this amount allows to observe gettering properties for O_2. After it was cleared that the gettering rate of O_2 is too slow, big isolation volume was replaced in small ones.

4.2.1.4. Gettering Tests for O_2 by Using Small Test Volume

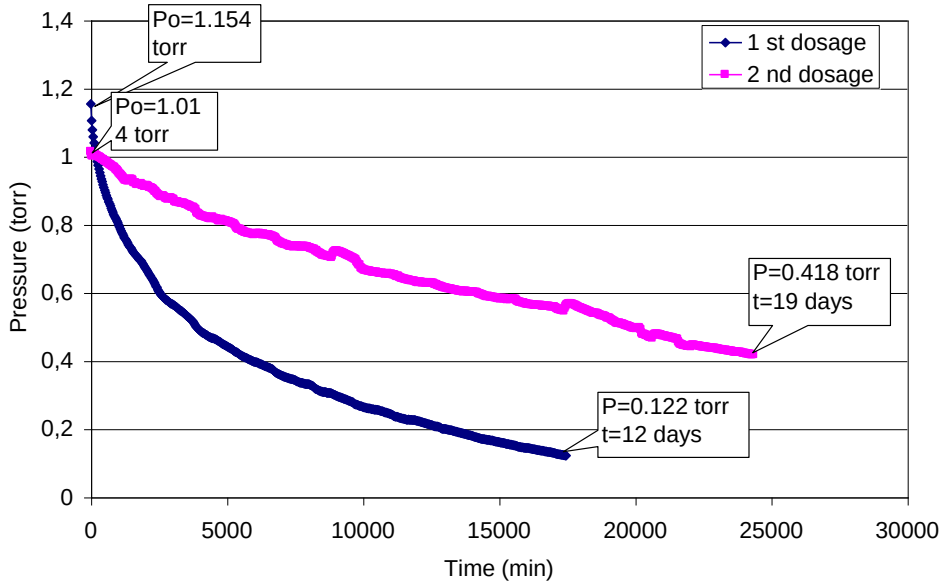

Figure 4.7: Pressure decrease observed in small isolated volume due to O_2 gettering ($V_{isolated}$=0.159 liter)

Due to the 2. test by big isolation volume, gettering capacity was calculated as 0.7 mbar*l, this value was achieved only by sending one gas dosage. The gettering capacities that were calculated are for 4.469 torr*l gas dosing. That means 4.469 torr*l gas is accumulated on getter by one gas dosage if big isolation volume was used. If the small isolation volume was used, the gas accumulated on getter would be around 0.159 torr*l. To determine total sorption capacity by small isolation volume, multiple dosages should sent on getter. Since it takes too much time to absorb all the sent gas by getter, tests with small volume were achieved only for two gas dosages. At the end of the first dosage the capacity received to 0.21 mbar*l. After second dosage total sorption capacity of getter was calculated as 0.34 mbar*l. These two tests continued 29 days. If total absorption capacity is accepted as 0.7 mbar*l, the test should be carried on about 30 days more to reach this value due to the equations 4.13 and 4.14.

$$0.7/0.34=59 \text{ days} \quad (4.13)$$

$$59 \text{ day} - 29 \text{ day} = 30 \text{ days} \quad (4.14)$$

Because the tests by small volume takes too much time, test was stopped and measured value (0.7 mbar*l) by big volume was accepted as total absorption capacity. This value was also confirmed by the manufacture of getters. Gettering rate that is seen in Figure 4.8 was accepted as $1.47*10^{-3}$ mbar*cc/sec.

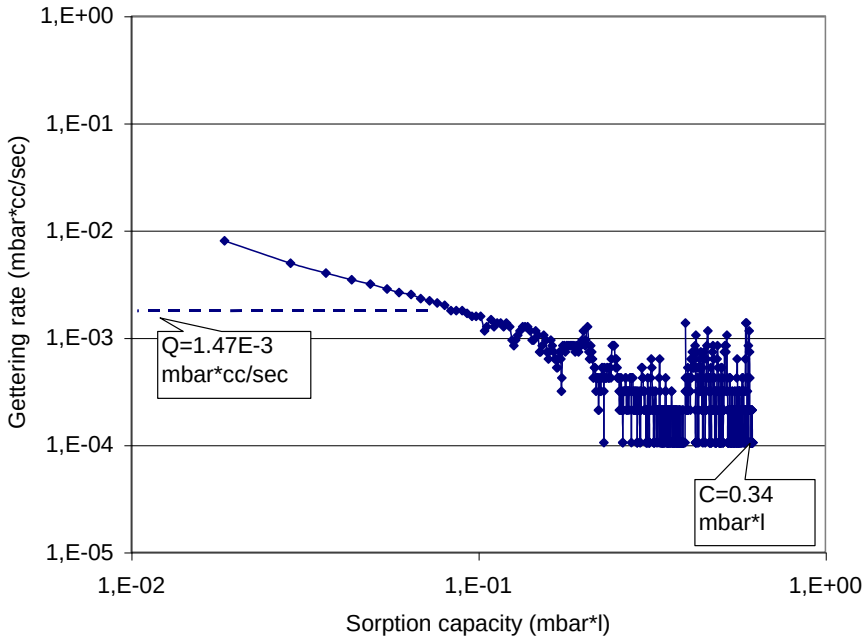

Figure 4.8: Gettering rate and sorption capacity of getter material for O_2 gas ($V_{isolated}$= 0.159 liter)

4.2.1.5. Gettering Tests for Air

The gettering tests for air were achieved by using both big and small isolation volumes. Gettering rate and total absorption capacity could not be measured by big volume by the same reasons as described in section 4.1.4 that is why it was replaced the smaller volume. In Figure 4.9 the pressure decrease, observed by big isolation volume is shown.

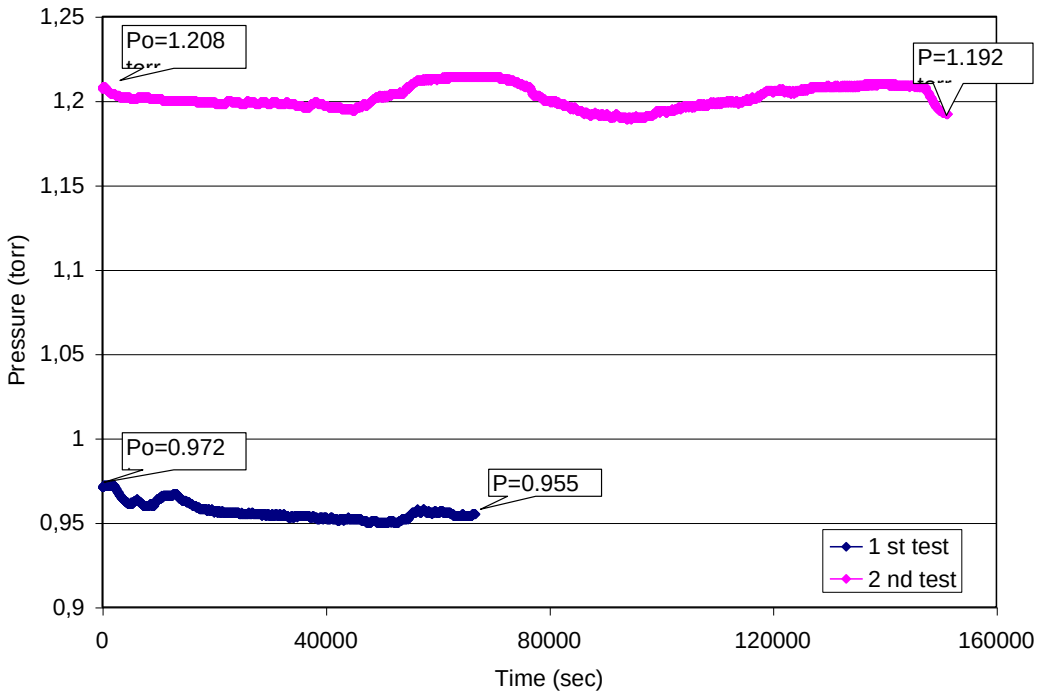

Figure 4.9: Pressure decrease observed in isolated volume due to air gettering (1.test, P_0= 0.971; 2.test, P_0= 1.207 torr; $V_{isolated}$=4.469 liter)

The percentage of N_2 in air mixture is 78%, where the percentage of O_2 is 21%. Related to these percentages it was expected that air gas should be absorbed by getter such N_2. Gettering tests for N_2 were achieved by sending 0.932 torr gas on getter. The pressure decrease due to N_2 absorption was completed at the end of 10140 minute. But for the same time duration, pressure decrease due to air absorption was only 0.017 torr. Tests were repeated with smaller isolation volume to decrease the gas amount sent on getter.

4.2.1.6. Gettering Tests for Air by Using Smaller Volume

By using small test volume air absoption was observed in two stages. The graph related to air absorption is shown in Figure 4.10. Pressure decrease due to air absorption maintained slowly until a sudden decrease. In the first stage O_2 gettering occurs, which was very slow. Second stage that begins by sudden pressure decrease was due to N_2 gettering. The reasons of these phenomena relate to the size of molecules and molecular interactions of O_2 and N_2. The bond length σ is 0.347 nm for O_2 while it is 0.380 for N_2. As an element, σ bond length of N is smaller than the bond length for O, but in molecular case N_2 will be larger, because its bond length will be longer than O_2. So, O_2 as a molecule has smaller size and it reaches to the free active sides of getter earlier than N_2. When O_2 reaches to the active sides it fills all the cavities on the surface and there will be no way to go through for N_2. This period can be called as “induction time” for N_2. After all the O_2 in the air mixture was absorped by getter, there occur some cavities on the surface of getter and N_2 can go through these cavities to the bulk of getter [18]. To fulfill the capacity of getter second and third dosages were sent on the same getter. But since it takes to long time to absorb all the sent gas, tests were stopped.

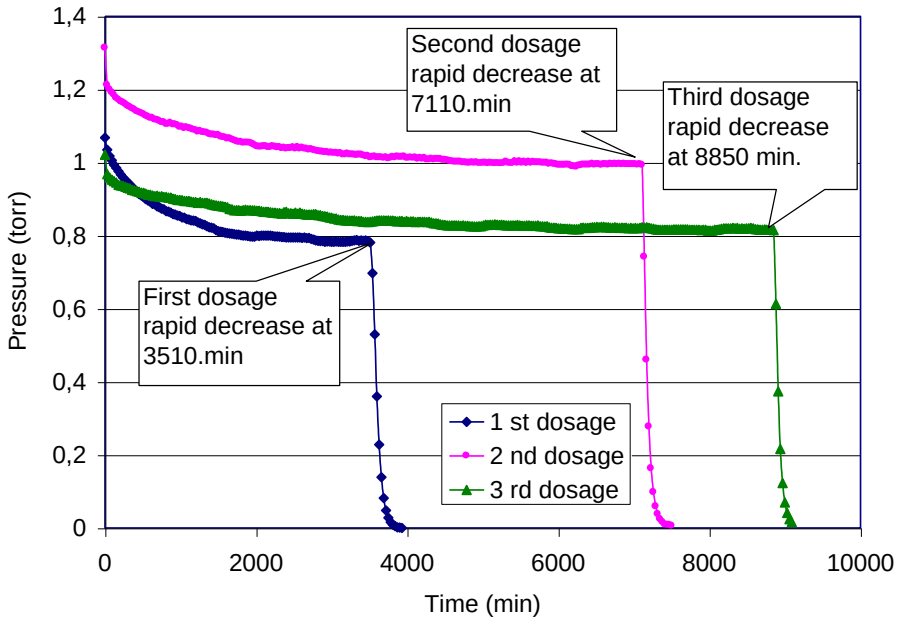

Figure 4.10: Pressure decrease observed in small isolated volume due to air gettering (P_0~1 torr; $V_{isolated}$= 0.159 liter)

According to Lennard-Jones equation, division of potential energy constant ε to the Boltzman constant k, gives the Lennard-Jones temperature (ε/k), expressed in Kelvin (K). This equation is related to polar interactions. Lennard-Jones temperature is 107 K for O_2, where it is 71 K for N_2. The interaction between gas and surface increases as the ratio ε/k increases. Thus, O_2 is adsorbed earlier than N_2, since it has higher ε/k value [17].

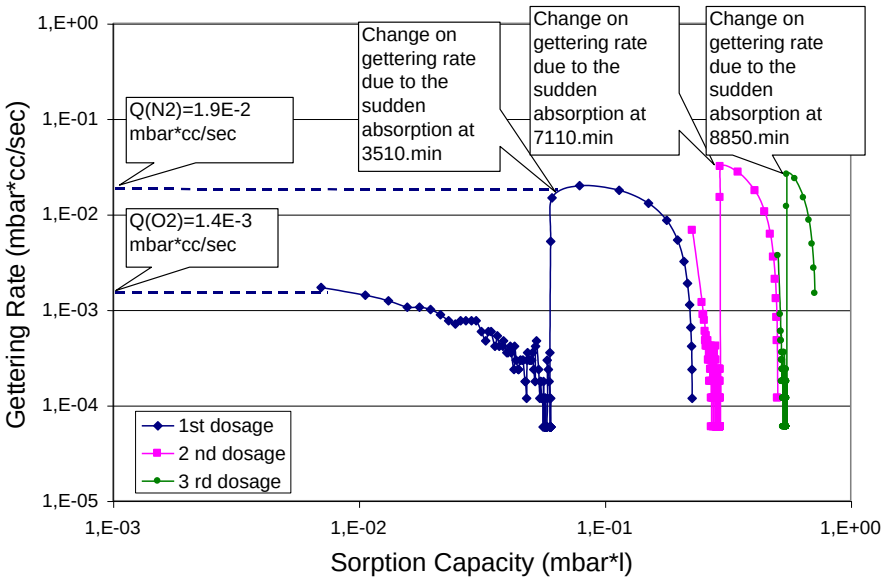

Figure 4.11: Gettering rate and sorption capacity of getter material for air (P_0 ~1 torr, $V_{isolated}$= 0.159 liter)

At second and third dosages, O_2 absorption takes much time than the previous dosage. This was the result of the number of free active sides that become less at

each dosage. O_2 covered most of the active sides on the surface. When new gas dosage was sent on the same getter, O_2 covered the free active sides. Therefore the number of free active sides reduced at each dosage. Because the number of active sides reduced, O_2 absorption get longer for each dosage. However N_2 absorption also get longer, because N_2 should go through O_2 molecules to reach to the bulk. Thus the O_2 amount on the surface increased, N_2 diffusion time also gets longer. As it can be seen in Figure 4.10, O_2 absorption maintained at first dosage 3510 min, while it get longer at second dosage, 7110 minute and much longer at third dosage, 8850 minute [18].

In Figure 4.11, the measured gettering rate from the beginning of the test until sudden pressure decrease related to O_2 was calculated as $1.4*10^{-3}$ mbar*cc/sec. Due to gettering test for O_2, described in section 4.1.3, gettering rate was found as $1.59*10^{-3}$ mbar*cc/sec, this two gettering rate results are very similar and it supports, that air absorption occurred firstly by O_2 absorption. Again in Figure 4.11, there is seen sudden increase at gettering rate. This was related to the N_2 adsorption. At first dosage gettering rate after sudden increase was determined $1.9*10^{-2}$ mbar*cc/sec, this result confirmed that it relates to N_2. Due to N_2 test, that was described in section 4.1.2, gettering speed was determined as $1.9*10^{-2}$ mbar*cc/sec. As in Figure 4.11, at second and third dosages gettering rates for O_2 slow down without being a constant value. The reason is the decrease in number of active sides, which were covered by O_2 and N_2 molecules at previous dosages.

O_2 adsorption occurs easily in the presence of N_2. N_2 reacts with surface of getter and this changes the morphology of the surface, so the surface area and number of active sides increases. This increase facilitates O_2 adsorption. Belong to this, there will a suddenly increase at gettering rate for second and third dosages. This increase is not continuous because there are less active sides to fill up. Therefore after a suddenly increase, gettering rate begins to slow down and cannot reach to a constant value. In Figure 4.11, suddenly increased gettering rate values are read as $6.74*10^{-3}$ mbar*cc/sec for second dosage and $3.6*10^{-3}$ mbar*cc/sec for third dosage. These two rate values are higher than the rate for first dosage.

When the sorption capacity for N_2 take in consideration, total capacity for N_2 should be at least 5.5 mbar*l. To reach this capacity value sorption test should be done by sending 26 dosages of gas. When large volume is used it is difficult to see the pressure decrease, because the amount of accumulated gas on getter will be to much.

4.2.2. Comparison of Absorption Characteristics for Various Gases on Getter

Gettering characteristics of a getter type for atmospheric gases like N_2, CO, CO_2, O_2 and air were investigated by sending ~1 torr of selected gas on getter material. Related to absorption of test gas by getter, pressure decrease was observed with respect to time. It was waited until all of the sent gas was absorbed by getter and pressure decrease stopped. The results are given in Figure 4.12 and Figure 4.13. The pressure decrease was observed due to the absorption of gases by $BaLi_4$ layer of getter. The results for N_2, O_2 and CO were achieved with 4.469 liter test volume, however the result for air is achieved with 0.159 liter test volume.

The most rapid pressure decrease was observed by absorption of CO and CO_2, while the decrease was slower for N_2. Pressure decrease due to O_2 absorption was the slowest among the tested gases. Air absorption was occurred in two stages. Pressure decrease due to air absorption maintained slowly until a sudden decrease. In the first stage O_2 gettering occurs, which was very slow. Second stage that begins by sudden pressure decrease was due to N_2 gettering as it was discussed in section 4.1.6.

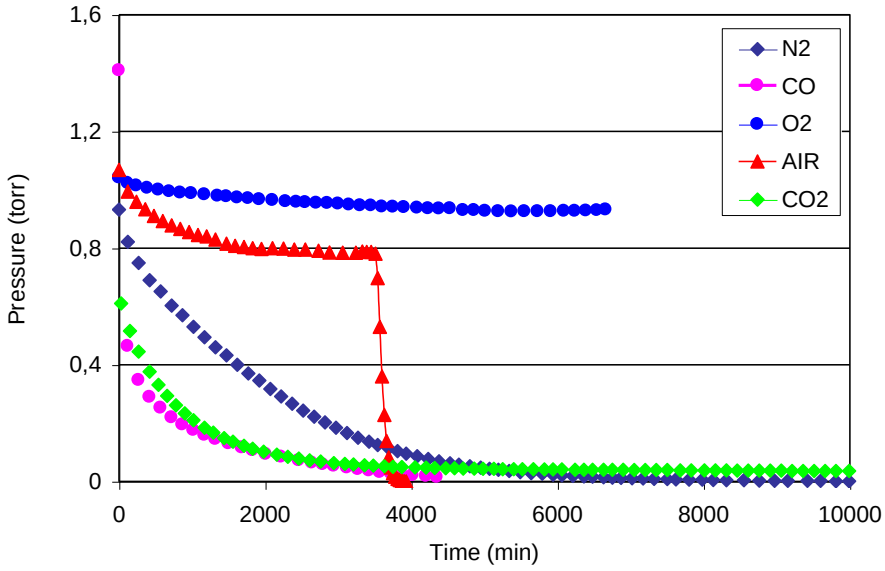

Figure 4.12: Pressure decrease observed in isolated volume due to gettering of various test gases ($P_0 \cong 1$ torr)

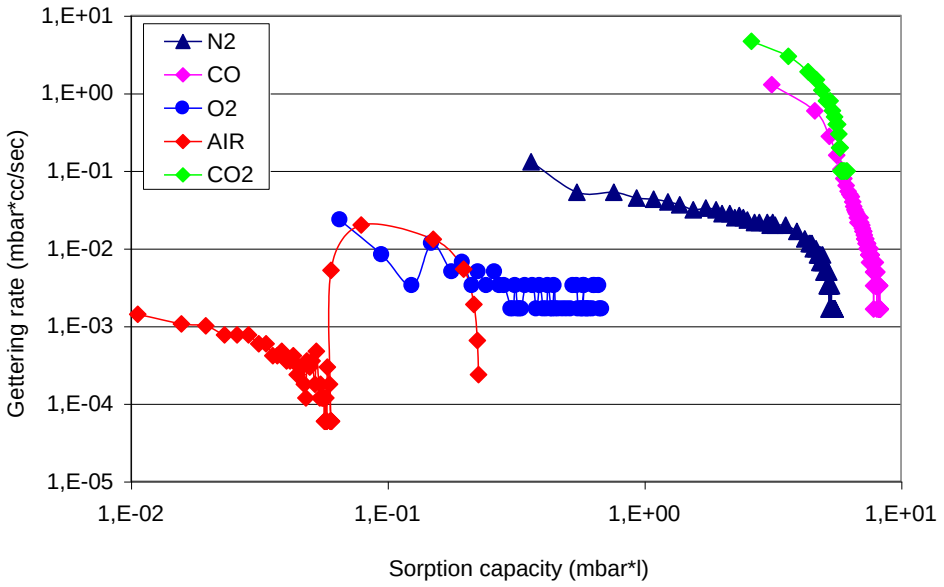

Figure 4.13: Gettering rate and sorption capacity of getter material for various gases ($P_0 \cong 1$torr)

As it can be seen in Figure 4.13, gettering rate slows down with respect to time, however it seems constant in the beginning. The curve where it seems constant can be accepted as gettering rate. Gettering rates of CO and CO_2 were determined to have the highest values, while N_2 gettering was slower than these two gases. O_2 gettering rate was the lowest. As it is described above, air gettering occurred in two steps. Firstly lower gettering rate was determined which is related to O_2 and then gettering occurred rapidly due to N_2 absorption.

The gettering capacities that were calculated in Figure 4.13 are for 4.469 torr*l gas dosing. That means 4.469 torr*l gas was accumulated on getter by one gas dosage. The highest capacity of getter was observed for CO and CO_2, where it was less for N_2. Gettering capacities for O_2 and air could not be calculated, because gettering rate of O_2 was very slow and it takes too much time to complete the test. All of the gettering capacity values, achieved among this study do not show the total capacity values, because only one gas dosage was sent on getter and it was not repeated again. The reason was that the gettering capacity values measured experimentally (at the end of first dosage) are sufficient to absorb all the gases accumulated in the panel during the lifetime of a VIP.

As a conclusion, getter material has different characteristics for various gases. The main properties to evaluate a getter are, gettering capacity and gettering rate. Among this study N_2, CO, CO_2 O_2 and air gases were tested and their gettering

properties were calculated. In Table 4.1 the results are given with the manufacturers specifications [17].

Table 4.1: Comparison of gettering capacity and gettering rates for various gases

	Gettering capacity	Gettering capacity	Gettering rate
GAS	Measured values (mbar*l)	Manufacturer's specification (mbar*l)	Measured values (mbar*cc/sec)
(N_2 +O_2)		>5.5	
N_2	>5.5	-----	$1.9*10^{-2}$
O_2	>0.7	-----	$1.6*10^{-3}$
(CO+CO_2)		>8.0	
CO_2	>6.0	-----	$6.6*10^{-2}$
CO	>8.3	-----	2.9
AIR	Tests are stopped	>5.5	----

4.2.3. Evaluation of Different Getter Types

Gettering properties of three different getter types were determined due to their gettering capacity and gettering speed, for various gases and the results were compared with each other.

4.2.3.1. Gettering Tests for N_2

To determine gettering properties for N_2, 1 torr test gas sent on getter material, then it was waited until the pressure decrease stops. Experimental parameters used in gettering tests and the results for gettering speed and gettering capacity are given in Table 4.2 [2]. The comparison of gettering properties for N_2 are shown in Figure 4.14. As it can be seen from the Figure, Getter A and Getter B have similar gettering

speeds. Getter C has significant lower gettering speed compared to the other two getters. However all three getter types have nearly the same gettering capacity values.

Figure 4.14: Gettering rate and sorption capacity of different getter materials for N_2

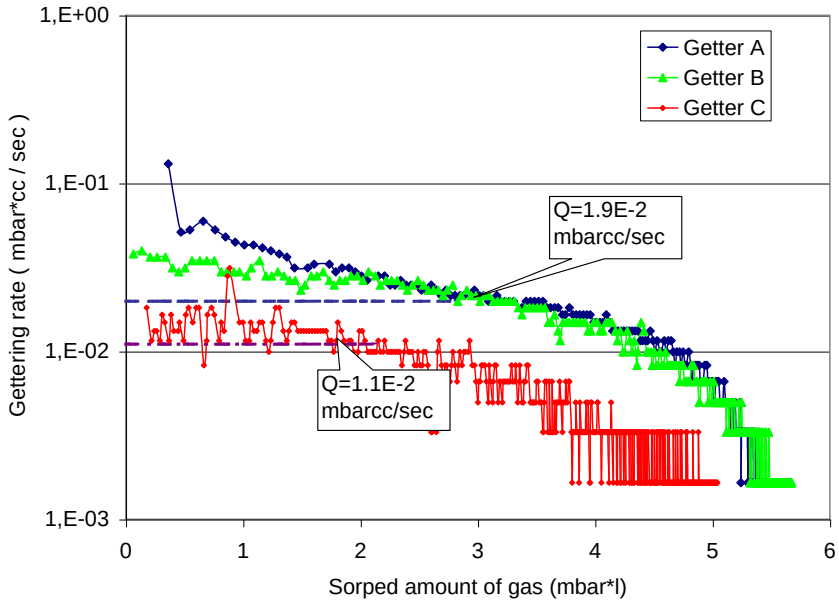

($P_0 \cong 1$torr)

Table 4.2: Process parameters and gettering results

	Getter Type		
	A	B	C
P_0 (torr)	0,932	0,954	1,218
P (torr)	0	0	0,406
$\Delta P=P_o-P$ (torr)	0,932	0,954	0,812
C (mbar*l)	5,53	5,6	5,0
Q (mbar*cc/sec)	1,9E-2	1,9E-2	1,1E-2

4.2.3.2. Gettering Tests for CO

Gettering characteristics for CO gas were also similar to N_2 results. Gettering speeds of Getter A and Getter B were overlapping, on the other hand, it is lower for Getter C. Their comparison can be seen in Figure 4.15.

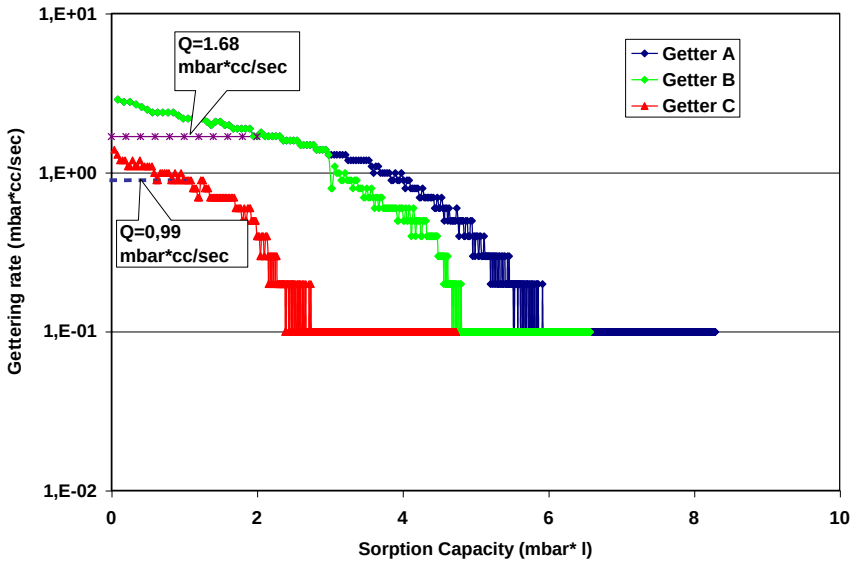

Figure 4.15: Gettering rate and sorption capacity of different getter materials for CO ($P_0 \cong 1$torr)

4.2.3.3. Gettering Tests for CO_2

Absorption characteristics of CO_2 are similar to CO. Getter A and Getter B absorb CO_2 faster than Getter C. Experimental results are given in Figure 4.16.

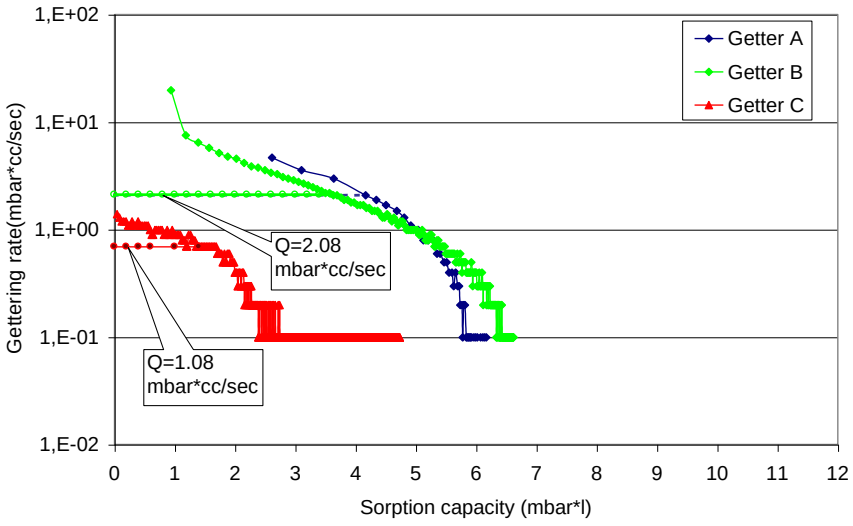

Figure 4.16: Gettering rate and sorption capacity of different getter materials for CO_2 ($P_0 \cong 1$torr)

Gettering speed of Getter A and B were overlapping on top of each other, on the other hand absorption speed of Getter C is again slower. The calculated gettering capacities of Getter A and B are also similar to each other. Getter C has relatively lower absorption capacity compared to A and B.

4.2.3.4. Gettering Tests for O_2

Pressure decrease with respect to time could not be observed during O_2 absorption tests. All the getter types were tested to determine pressure decrease due to O_2 absorption, however the decrease was too slow that it can be assumed as there is no decrease in pressure. As a result of slow pressure decrease, gettering rate and gettering capacity could not be determined. In Figure 4.17, pressure decrease of O_2 is given. But this study gives an idea about absorption characteristics of O_2.

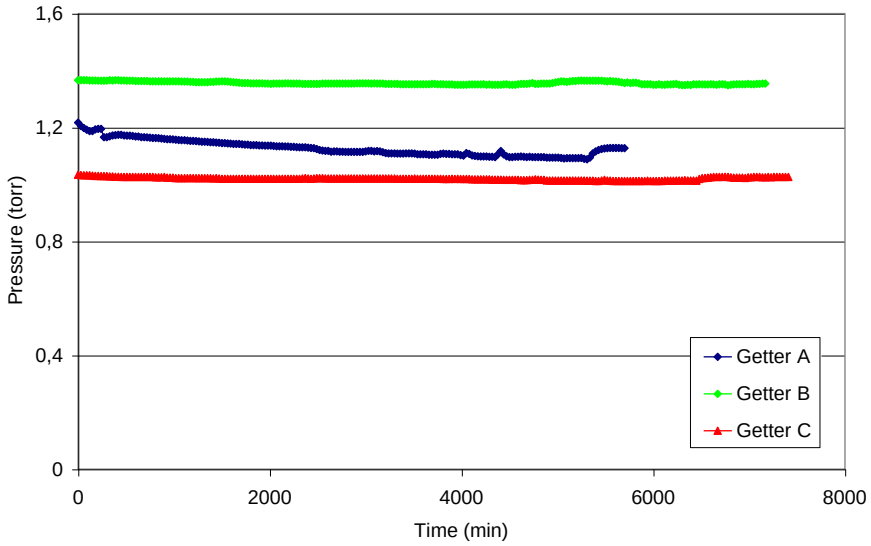

Figure 4.17: Pressure decrease due to O_2 gettering for different getter types ($P_0 \cong 1$ torr)

The amount of chemical ingredients of the Getter Materials decreases in the order of Getter A>Getter B>Getter C. As it is seen in Table 4.3, Getter A and Getter B have nearly the same gettering rates for the tested gases, however Getter C has a lower gettering rate. Gettering capacities are similar in Getter A and Getter B, while it is less for Getter C. Even though Getter C has the lowest gettering capacity, its capacity is still enough to absorb all the accumulating gases in the panel. The amount of gases accumulated in the panel during its lifetime was investigated by VACSIM program.

Table 4.3: Comparison of gettering properties of different getter types

	Q (mbar*cc/sec)			C (mbar*l)		
	Getter A	Getter B	Getter C	Getter A	Getter B	Getter C
N_2	0.019	0.019	0.011	5.5	5.5	5.0
CO	1.7	1.7	0.9	8.3	6.6	4.7
CO_2	2.1	2.1	1.1	6.1	6.6	4.7
O_2	*			0.7	*	*

*Could not be determined

4.3. Evaluation of Getter Materials by VACSIM

To evaluate the usage of a getter system, pressure changes of four different vacuum panels were measured due to time by spirotorr vacuum gauge and the results were compared with the theoretical results. The panels were consisting of different inner filler materials with and without getter material. The dimensions, first pressure values and critical pressures of the panels are given in Table 4.4.

The pressure increases in VIPs with getter material were less than the pressures in the panels without a getter. The comparison of panels can be seen in Figure 4.18. At the end of 400 days pressure increase was observed as 0.181 mbar and 0.172 mbar in the panels (XPS-NG, OCPU-NG) without a getter, where it was 0.0304 mbar and 0.0278 mbar in the panels, (XPS-G, OCPU-G) with a getter material [4].

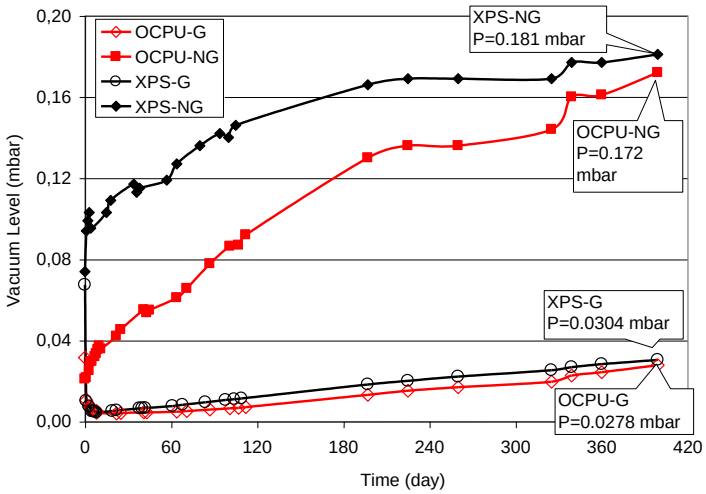

Figure 4.18: Comparison of pressure increases between VIP s with or without getter material

Table 4.4: Properties of evaluated VIPs

VIP type	PANEL DIMENSIONS(cm)			FLANGE DIMENSIONS(cm)					
	Height	**Width**	**Length**	**1**	**2**	**3**	**4**	**P_0(mbar)**	**P_c(mbar)**
OCPU-G*	51,2	34,7	2,5	2,4	5,4	2,3	2,4	0,0315	0,05
OCPU-NG*	51,4	34,7	2,5	2,4	5,2	2,2	1,9	0,021	
XPS-G	52,1	35,0	2,5	1,9	5,5	2,0	1,9	0,0154	0,2
XPS-NG	52,1	34,7	2,5	2,6	5,2	2,2	1,7	0,0476	

G*: With getter material

NG*: Without getter material

OCPU: Open cell polyurethane

XPS: Extruded polystyrene

P_0: Pressure value measured just after evacuation process

P_c: Critical pressure value

To check the reliability of the simulations, experimental results were compared with theoretical results that were calculated by VACSIM simulation program. The comparison of experimental and theoretical results for vacuum level change in the panels with open celled XPS inner filler material and a getter material is given in Figure 4.19. In Figure 4.20 the comparison is given for the panel with the same inner filler material without a getter material.

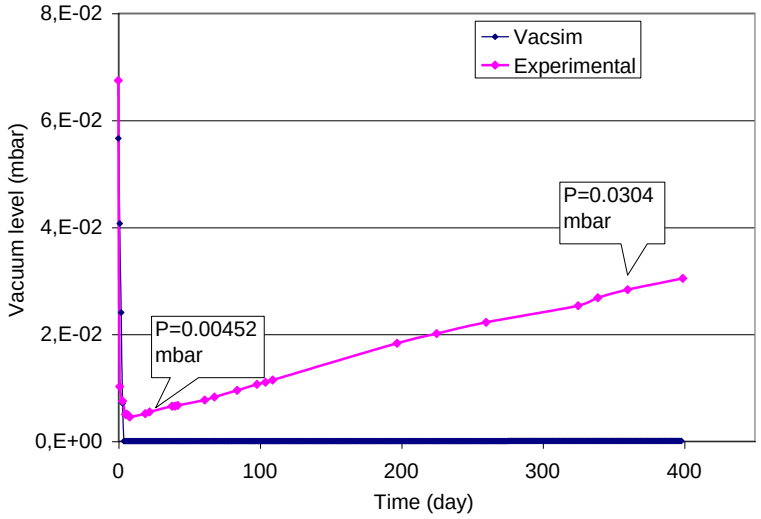

Figure 4.19: Comparison of experimental results to VACSIM simulation due to pressure increase in XPS panel with getter

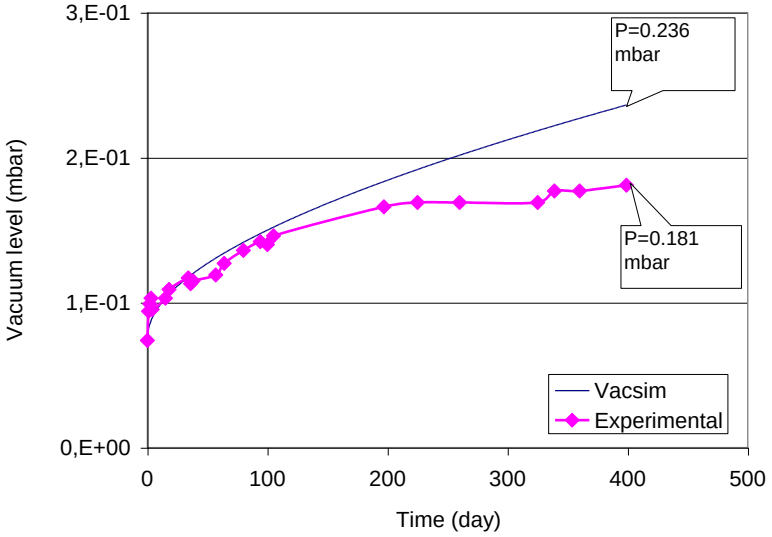

Figure 4.20: Comparison of experimental results to VACSIM simulation due to pressure increase in XPS panel without getter

Another comparison was made for the panels including OCPU as inner filler material with and without getter material. In Figure 4.21 and Figure 4.22, comparisons due to pressure increases are given for these panels.

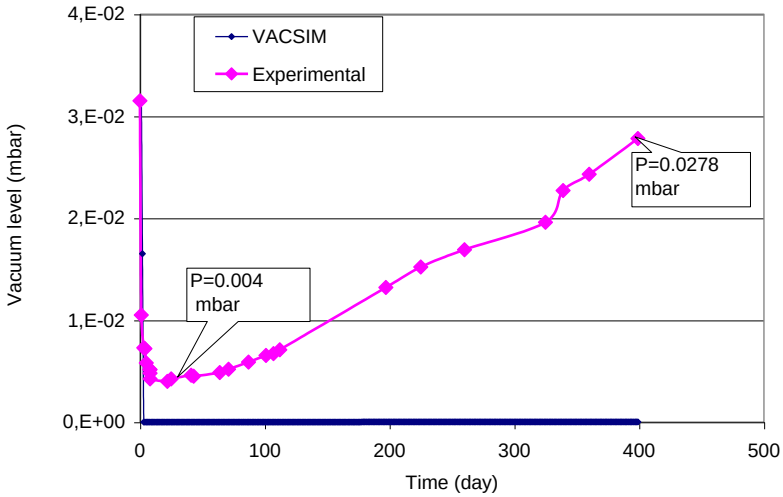

Figure 4.21: Comparison of experimental results to VACSIM simulation due to pressure increase in OCPU panel with getter

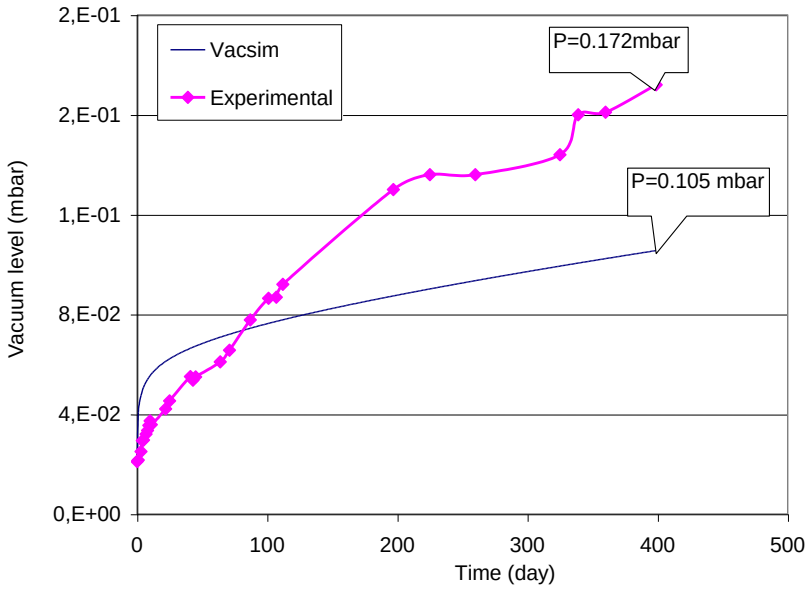

Figure 4.22: Comparison of experimental results with VACSIM simulation due to pressure increase in OCPU panel without getter

The comparisons show that simulation results are in good correlation with experimental results. This shows that vacuum level at any desired time can be predicted by using VACSIM simulation program. When a getter is used, the predictions of VACSIM deviate from the experimental values in that an increase is observed for both panels whereas VACSIM predicts no pressure increase taking into consideration the gettering capacity of the getter. This deviation may arise from the unforeseen leaks in sealing flanges and/or sealing zone around spirotorr.

VIPs with getter material were evaluated by VACSIM simulation program for 20 years. The amount of each gas that will accumulate in the panel was calculated and the result was compared with the capacity of getter material. It was seen that the

capacity of the getter is sufficient to absorb all the gases in the panel that were collected in 20 years. The comparison is given in Table 4.5.

Table 4.5: Comparison of gettering capacity to the amount of gas that was accumulalated in the panel in 20 years

	Gettering Capacity (mbar*l)	Total amount of gas accumulated inside the panel in 20 years (mbar*l)	
GAS		**OCPU - G**	**XPS - G**
CO	8.4	0.15	0.98
CO_2	6	0.14	0.26
O_2	0.7	0.31	0.36
N_2	5.5	1.14	2.15
CH_4	1.33	$8.8*10^{-4}$	--------
H_2	93.32	----------	0.26
H_2O	799	0.19	0.19

VIP Dimensions: (51cmx34cmx2.5cm)

4.4. Evaluation of Theoretical Calculations for VIC Applications

Barrier material used in VIC applications can be either multilayer or monolayer structure. The structure properties strongly affect the permeability of barrier material. By using VACSIM-VIC program, pressure increase with respect to time can be estimated. The VIC cabinet, studied on, is shown in Figure 4.23.

Figure 4.23: VIC cabinet

In this thesis, different multilayer structures were investigated for this VIC for desired conditions and the most convenient structure was determined. After this determination, it was studied on determination of the optimum thickness of the best structure. Pressure increase in ten years should not exceed the critical pressure of inner filler material. Thermal conductivity is independent from the pressure until

pressure reaches to critical value. Over critical pressure value, insulation property of VIC is deteriorated. It was assumed by simulations, that the inner filler material of the VIC is fumed silica. Thermal conductivity value of fumed silica is 5 W/ mK at 10 mbar that is the critical pressure value. At 100 mbar the thermal conductivity raises to 8 W/mK. Thus, its critical pressure can be considered as 100 mbar. Critical pressure of an inner filler material can be determined by S-curves, the S-curve of fumed silica is given in Figure 4.27 [3]. In the curve, the thermal conductivity seems constant at the beginning, however it begins to increase after some time. The point when the increase begins, is the critical pressure value.

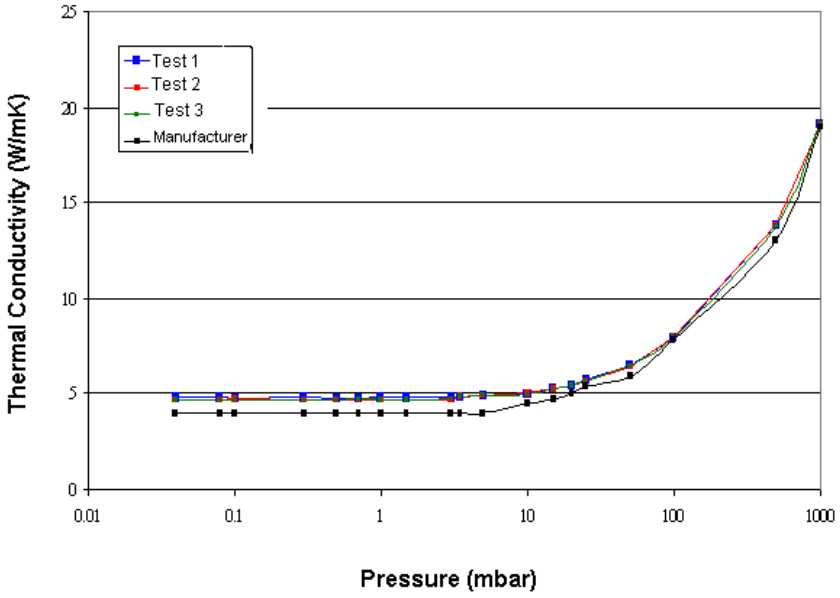

Figure 4.24: S-curve of fumed silica

The best multilayer structure was determined by changing the cabinet conditions for three different systems. In Table 4.6, the structures of the studied multilayer plastic barriers are given.

Table 4.6: Studied multilayer structures

	Inner barrier plastic	Thickness (mm)	Outer barrier plastic	Thickness (mm)
1	HIPS / EVOH	1/0.1	HIPS / EVOH	1/0.1
2	HIPS	1.5	HIPS/EVOH	2/0.05
3	ABS/EVOH	1/0.1	ABS/EVOH	1/0.1
4	ABS	1.5	ABS/EVOH	2/0.05
5	HDPE/HIPS/WS	0.3/0.4/0.8	HIPS/WS/HDPE	0.3/0.4/1.3
6	ABS	1.5	PMMA/ABS/WS	1/0.5/ 0.01
7	ABS	2.6	ABS/PMMA	2.6/ 0.1
8	ABS/HDPE	2.6/0.2	PMMA/ABS/HDPE	2.6/0.2/0.1
9	ABS/WS/EVOH	0.8/0.7/0.05	ABS/WS/EVOH	1/1/0.05
10	ABS	2.6	PMMA/ABS/HDPE	2.6/0.2/0.1
11	ABS/WS	2.6/0.2	PMMA/ABS/WS	2.6/0.2/0.1
12	ABS/WS	0.14/2.47	PMMA/ABS/WS	0.14/2.47/0.29
13	WS/HDPE	2.6/0.2	PMMA /WS/HDPE	2.6/0.2/0.1
14	ABS/WS	0.8/0.7	ABS/WS/EVOH	1/1/0.05

These structures were evaluated by VACSIM-VIC program to determine the most convenient one that causes minimum pressure increase in 10 years. For the first system; the parameters used in calculations are given in Table 4.7. The temperature conditions are representing the fresh-food part of refrigerator. Detailed descriptions of parameters were given in section 2.3.2.7.

Table 4.7: Parameters used in simulations for system 1

V	22 lt
t (air)	10 year
t (WV)	10 year
P_0 (air)	0 bar
P_0 (WV)	0 bar
$P_{ff/frz}$ (air)	1.013 bar
P_{out} (air)	1.013 bar
P (5^0C) (WV)	0.00435bar
P (25^0C)(WV)@%50	0.01585 bar
T_{in}	5^0C
T_{out}	25^0C
A_{in}	0.7 m^2
A_{out}	1.1 m^2
T(temperature of insulation volume)	18^0C
$P_{sat-WVT}$@18^0C	20.634
RH@25^0C	%50

Structures were compared with each other, related to pressure increase in 10 years as it is shown in Figure 4.25. For this step, critical pressure is not taken in consideration, but the study was focused on determination of the barrier structure.

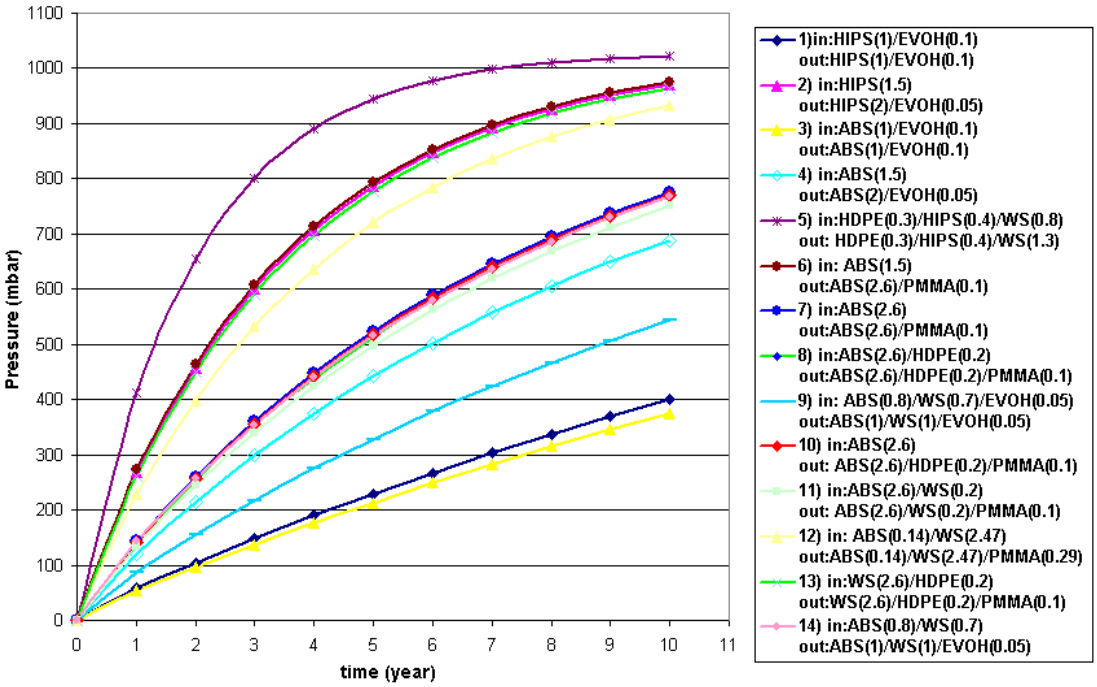

Figure 4.25: Pressure increases with respect to time for different barrier structures in system1(Thicknesses are given in mm unit)

Numeric values about pressure increase for these structures are given in Table 4.8. P_T columns are representing the gas permeability values of multilayer structures, where $WVTR_T$ columns are the permeability values for water vapor related to inner and outer temperature conditions. The pressure increases related to air diffusion and water vapor permeation and total pressure increases are also given in Table 4.8.

Table 4.8: Permeability values of different type of multilayer structures and the pressure increases in the freshfood

Structure number	$P_{T\,in}$ (cm^3/m^2*day*bar)	$P_{T\,out}$ (cm^3/m^2*day*bar)	$WVTR_{T\,in}$ (g/m^2*day*bar)	$WVTR_{T\,out}$ (g/m^2*day*bar)	Pressure Increase related to air permeation (mbar)	Pressure Increase related to WV permeation (mbar)	Total Pressure Increase (mbar)
1	0.9	2.0	45.8	38.8	390.3	15.85	401.1
2	18.6	3.6	91.6	36.0	955.1	15.85	970.9
3	0.8	1.8	43.0	39.2	364.3	15.85	380.2
4	5.0	2.7	76.4	36.7	673.1	15.85	688.9
5	10.6	20.1	0.8	4.3	1006.0	15.85	1021.8
6	5.0	12.6	76.4	27.5	958.3	15.85	974.1
7	2.8	5.6	44.1	35.6	768.9	15.85	784.7
8	2.7	5.5	4.2	7.4	749	15.85	764.8
9	1.5	3.0	1.2	14.2	528.7	15.85	544.5
10	2.8	5.5	44.1	7.4	753	15.85	768.8
11	2.7	5.4	4.1	25.9	746	15.85	761.8
12	5.2	9.2	0.3	7.1	913	15.85	928.8
13	3.0	12.4	0.1	4.0	946	15.85	961.8
14	6.4	3.2	1.2	19.0	752.0	15.85	767.8

The best structure for a desired VIC, has the lowest permeability value, and related to this result, the lowest total pressure increase occurs. This structure is found as the third structure. If this structure is used as barrier material, the pressure increase on insulation volume will be 364 mbar at the end of 10 year. Maximum pressure increase caused by water vapor can reach to 15.85 mbar at 25^0C and 50%RH.

Water vapor pressure in the cabinet is 4.35 mbar at 5^0C and 50%RH conditions and it is 15.83 mbar at outside conditions, that is 25^0C and 50%RH. If insulation volume assumed as fully evacuated, pressure at the beginning will be 0 mbar, thus water vapor diffusion occurs from inner and outer part to the insulation volume of cabinet. Afterwards, pressure on insulation volume will be equal to the pressure at the inner part of cabinet. After this point, pressure on insulation volume will be higher than the pressure at the inner part, because of the diffusion continues from the outer part. Maximum pressure value on insulation volume at 18^0 C, can be 20.6 mbar. This value is higher than the pressure value at outside conditions that is why there is no condensation on insulation volume. Related to the pressure differences between inside and outside conditions of cabinet, pressure value on insulation volume cannot exceed 10.73 mbar.

As it is seen in Figure 4.27, the best structure consists of 1mm Acrylonitrile butadiene styrene (ABS)+0.1mm Ethylenevinylalcohol (EVOH). The nearest possible structure to this structure consists of 1mm High Impact Polystyrene (HIPS) +0.1mm EVOH. Pressure increase related to gas diffusion is 390 mbar and 364 mbar as they are seen in Table 4.7. Water vapor diffusion causes a pressure increase as 15.83 mbar for both of the structures and the rest was due to air permeation.

One of the most important parameters by vacuum simulation that should be taken in consideration is the critical pressure value of inner filler material. For fumed silica critical pressure value is 100 mbar. So, the thickness of most convenient structure is determined that does not allow to exceed the critical pressure value. The structures that cause minimum pressure increase are given in Table 4.9 with their thicknesses and they are compared on a graph with each other in Figure 4.26.

Table 4.9: The structures studied on for thickness optimization (system 1)

	Inner Plastic	Thickness(mm)	Outer Plastic	Thickness(mm)
1	ABS/WS/EVOH	0.8/0.7/0.05	ABS/WS/EVOH	0.8/0.7/0.5
2	ABS/WS/EVOH	0.8/0.7/0.1	ABS/WS/EVOH	0.8/0.7/0.5
3	ABS/WS/EVOH	1/0.7/0.1	ABS/WS/EVOH	1/0.7/0.5
4	ABS/EVOH	1/0.1	ABS/EVOH	2/0.5
5	ABS/EVOH	1.5/0.15	ABS/EVOH	2/0.5
6	ABS/EVOH	1.5/0.2	ABS/EVOH	2.5/0.5
7	ABS/EVOH	1.5/0.25	ABS/EVOH	2.5/0.5
8	ABS/EVOH	1.5/0.25	ABS/EVOH/PMMA	2.5/0.5/0.1
9	ABS/EVOH	1.5/0.3	ABS/EVOH	3/0.5
10	ABS/EVOH	1.2/0.6	ABS/EVOH	3/0.6
11	ABS/EVOH	1.4/0.4	ABS/EVOH	3/0.5
12	ABS/EVOH	1.5/0.4	ABS/EVOH	3.1/0.5
13	ABS/EVOH	1.8/0.4	ABS/EVOH	2.7/0.6

The parameters used for determining optimum multilayer structure are similar with the parameters used for the optimum thickness computations.

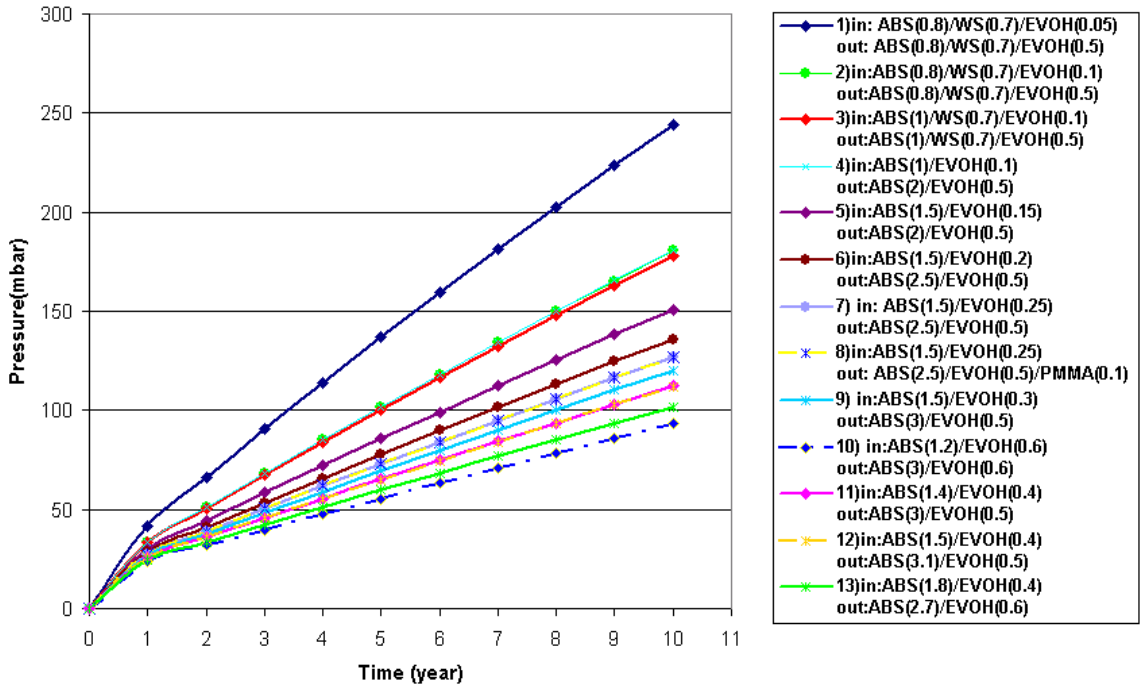

Figure 4.26: Pressure increase with respect to time for different thicknesses of the structures (system 1)(Material thicknesses are given in mm unit)

The best structure was determined as 3 mm ABS+ 0.6 mm EVOH for outer barrier material, where it was 1.2 mm ABS+ 0.6 mm EVOH for the inner barrier material,

that is shown with number 10 in Figure 4.26. If these structures are used, pressure increase will be 93 mbar at the end of 10 year. This pressure value is less than the critical pressure value of fumed silica. An alternative to this structure can be given as 2.7 mm ABS+0.6 mm EVOH for outer barrier; and 1.8 mm ABS+ 0.4 mm EVOH for inner barrier material, that is shown as number 13 in Figure 4.26. By this alternative structure pressure value reaches to 101 mbar at the end of 10 year.

The time duration for the vacuum level inside the cabinet to reach a value of 100 mbar can be easily found from Table 4.10.

Table 4.10: Pressure increases for each year of studied structures until the end of 10 year (System 1)

TIME (year)	NUMBER OF STRUCTURE													PRESSURE INCREASE (mbar)
	1	2	3	4	5	6	7	8	9	10	11	12	13	
0	0	0	0	0	0	0	0	0	0	0	0	0	0	
1	41.3	33.6	33.3	33.6	30.2	28.5	27.5	27.5	26.7	23.8	25.9	25.8	24.7	
2	66.2	51.1	50.5	51.1	44.3	41.0	39.1	39.1	37.6	31.8	35.8	35.8	33.6	
3	90.5	68.3	67.5	68.3	58.3	53.4	50.5	50.5	48.3	39.7	45.7	45.6	42.4	
4	114.1	85.1	84.1	85.2	72.1	65.7	61.8	61.8	58.9	47.6	55.5	55.4	51.1	
5	137.1	101.7	100.5	101.8	85.6	77.7	73.0	73.0	69.3	55.4	65.2	65.0	59.8	
6	159.6	118.0	116.5	118.1	99.0	89.7	84.1	84.0	79.7	63.1	74.7	74.6	68.3	
7	181.5	134.0	132.3	134.1	112.2	101.5	95.0	94.9	89.9	70.8	84.2	84.1	76.8	
8	202.8	149.7	147.8	149.9	125.2	113.1	105.8	105.7	100.1	78.4	93.6	93.4	85.2	
9	223.6	165.2	163.1	165.4	138.0	124.6	116.5	116.4	110.1	85.9	102.9	102.7	93.6	
10	243.9	180.4	178.1	180.5	150.7	135.9	127.0	126.9	120.0	93.4	112.1	111.9	101.8	

A second simulation was performed for the freezer part. In this second simulation the VIC dimensions and the multilayer structures, are same as the first simulation, which was already described in section 4.5. The only difference between the first and the second simulations is the environmental conditions and are shown in Table 4.11.

Table 4.11: Parameters used in simulations for system 2

V	22 lt
t (air)	10 year
t (WV)	10 year
P_0 (air)	0 bar
P_0 (WV)	0 bar
$P_{ff/frz}$ (air)	1.013 bar
P_{out} (air)	1.013 bar
P (5^0C) (WV)	0.00075bar
P (25 ^{0}C)(WV)@%50	0.01585 bar
T_{in}	-18^0C
T_{out}	25 ^{0}C
A_{in}	0.7 m^2
A_{out}	1.1 m^2
T(temperature of insulation volume)	3.5^0C
$P_{sat-WVT}$@18^0C	20.634
RH@25^0C	%50

Water vapor pressure at –18^0C& 50%RH is 0.7 mbar, where it is 15.83 mbar for outside conditions. It is assumed that the insulation volume was completely evacuated, that is why pressure is taken as 0 mbar on insulation volume at the beginning. Thus water vapor diffusion occurs from the outside and the inside of refrigerator into the insulation volume. If the temperature of insulation volume is accepted as 3.5^0C, pressure level at 100%RH will be 7.85 mbar. Diffusion continues until to reach this pressure value. 7.85 mbar is the saturation pressure for this system and if it is exceeded, there will be no more pressure increase, however water vapor condensation occurs.

Related to given parameters, pressure increases as a function of water vapor diffusion and gas diffusion are calculated by VACSIM-VIC program. Results are given in Table 4.12.

Table 4.12: Permeability values and pressure increases of different type of multilayer structures in the freezer part

Structure number	$P_{T\,in}$ (cm^3/m^2*day*bar)	$P_{T\,out}$ (cm^3/m^2*day*bar)	$WVTR_{T\,in}$ (g/m^2*day*bar)	$WVTR_{T\,out}$ (g/m^2*day*bar)	Pressure increase related to air permeation (mbar)	Pressure increase related to water vapor permeation (mbar)	**Total Pressure Increase (mbar)**
1	0.4	2.0	56.3	38.9	344.3	15.16	359.4
2	8.2	3.6	138.8	36.0	815.6	15.16	830.9
3	0.3	1.8	48.6	39.2	320.5	15.16	335.7
4	1.8	2.7	87.8	36.7	522.6	15.16	537.8
5	2.3	20.1	0.02	4.3	994.4	15.16	1009.5
6	1.8	12.6	87.8	27.5	934.1	15.16	949.2
7	1.1	5.7	50.6	35.7	706.7	15.16	721.8
8	0.9	5.6	1.8	7.5	695.4	15.16	710.6
9	0.6	3.0	0.02	14.2	470.1	15.16	485.3
10	1.1	5.5	50.6	7.4	700.7	15.16	715.9
11	1.0	5.6	0.07	25.9	694.2	15.16	709.3
12	1.6	10.5	0.006	7.1	893.4	15.16	908.5
13	1.4	12.0	0.006	4.0	920.4	15.16	935.6
14	2.2	3.0	0.02	14.2	569.2	15.16	584.3

As it can be seen in Table 4.12 the best structure is number 3, which allows the minimum pressure increase in 10 years. This structure is again 1 mm ABS+0.1 mm EVOH for both inner and outer barriers as in freshfood simulation. An alternative structure can be given as 1 mm HIPS+0.1 mm EVOH that is given by number 1.

In Figure 4.27, pressure increases related to multilayer structures are compared with each other for 10 years.

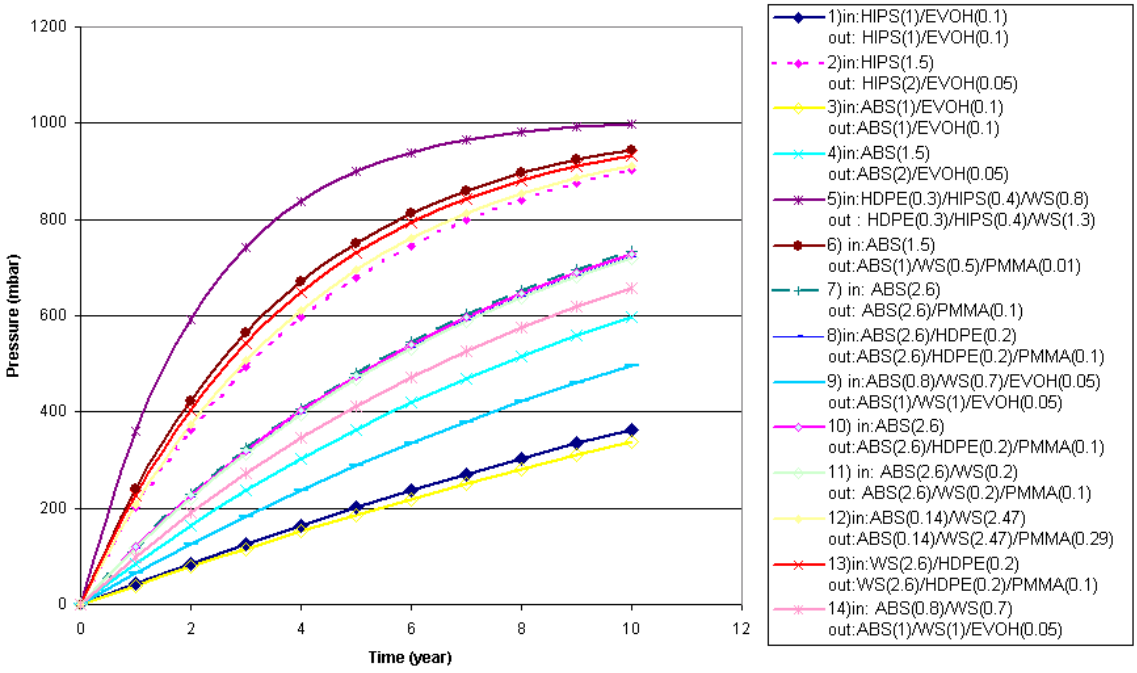

Figure 4.27: Pressure increases with respect to time for different barrier structures in system2 (Thicknesses are given in mm unit)

After determination of the best structure, thickness optimization was achieved for the structures given in Table 4.13.

Table 4.13: The structures studied on for thickness optimization (system 2)

	Inner Plastic	Thickness(mm)	Outer Plastic	Thickness (mm)
1	ABS/WS/EVOH	0.8/0.7/0.05	ABS/WS/EVOH	0.8/0.7/0.5
2	ABS/WS/EVOH	0.8/0.7/0.1	ABS/WS/EVOH	0.8/0.7/0.5
3	ABS/WS/EVOH	1/0.7/0.1	ABS/WS/EVOH	1/0.7/0.5
4	ABS/EVOH	1/0.1	ABS/EVOH	2/0.5
5	ABS/EVOH	1.5/0.15	ABS/EVOH	2/0.5
6	ABS/EVOH	1.5/0.2	ABS/EVOH	2.5/0.5
7	ABS/EVOH	1.5/0.25	ABS/EVOH	2.5/0.5
8	ABS/EVOH	1.5/0.25	PMMA/ABS/EVOH	2.5/0.5/0.1
9	ABS/EVOH	1.5/0.3	ABS/EVOH	3/0.5
10	ABS/EVOH	1.4/0.4	ABS/EVOH	3/0.5
11	ABS/EVOH	1.5/0.4	ABS/EVOH	3.1/0.4

Comparison of structure thicknesses is given in Figure 4.28. The structures that are near or below 100 mbar are appropriate as barrier material if fumed silica is used as inner filler material.

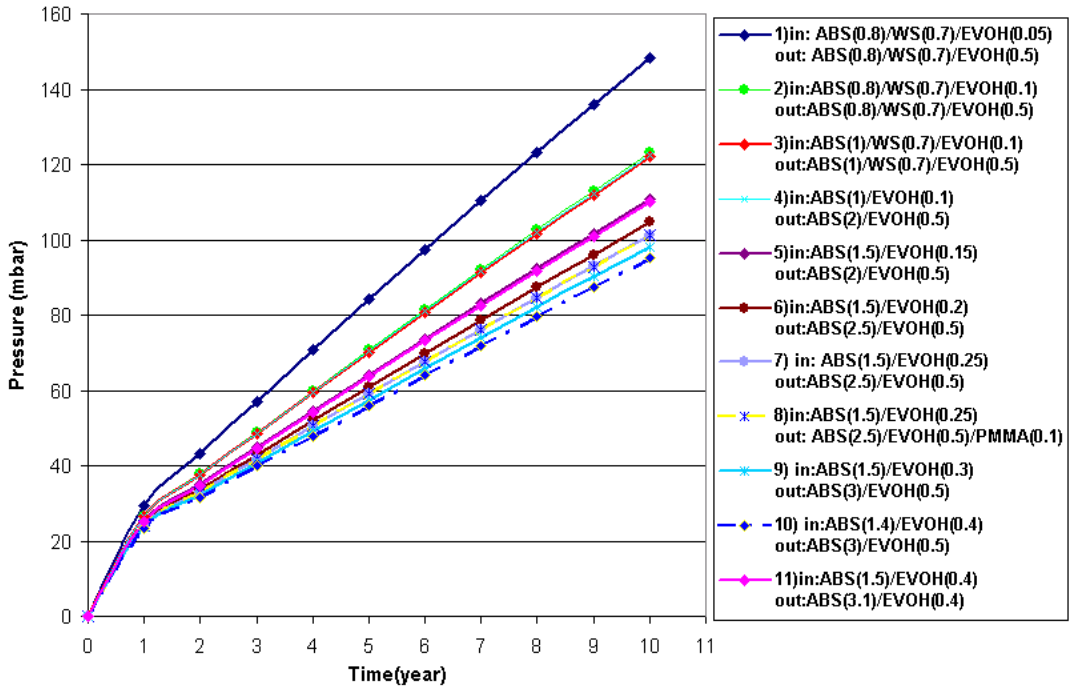

Figure 4.28: Pressure increase with respect to time for different thicknesses of the structures (system 2) (Material thicknesses are given in mm unit)

It was studied on 11 different structures for freezer part to determine the most appropriate thickness. The structure shown by number 10, that is 1.4 mm ABS+0.4 mm EVOH for inner plastic and 3 mm ABS+0.5mm EVOH for outer plastic is determined to be the most appropriate one. If this structure is used as barrier material, the pressure increase will be 95.11 mbar at the end of 10 year. This value does not exceed the critical pressure value of fumed silica. An alternative structure can be given by number 9, that is 1.5 mm ABS +0.3 mm EVOH for inner plastic and 3 mm ABS+0.5 mm EVOH for outer plastic. Pressure increase at the end of 10 year will be 98.1 mbar by using this structure. The time duration for the vacuum level inside the cabinet to reach a value of 100 mbar can be easily found from Table 4.14. In Table 4.14, pressure increases related to structure are given for each year.

Table 4.14: Pressure increases for each year of studied structures until the end of 10 year (System 2)

TIME (YEAR)	NUMBER OF THE STRUCTURE											
	1	2	3	4	5	6	7	8	9	10	11	PRESSURE INCREASE
0	0	0	0	0	0	0	0	0	0	0	0	
1	29.3	26.6	26.4	26.4	25.1	24.5	24.1	24.1	23.7	23.5	25.0	
2	43.3	37.7	37.5	37.6	35.1	33.7	33.0	32.9	32.3	31.6	34.8	
3	57.0	48.8	48.5	48.6	44.8	42.9	41.8	41.7	40.8	39.8	44.6	
4	70.6	59.8	59.4	59.5	54.6	51.9	50.5	50.4	49.2	47.9	54.2	
5	84.1	70.7	70.1	70.4	64.2	60.9	59.1	59.1	57.5	55.9	63.7	
6	97.3	81.4	80.7	81.0	73.7	69.8	67.7	67.6	65.8	63.9	73.2	
7	110.3	92.0	91.2	91.6	83.1	78.6	76.2	76.1	73.9	71.8	82.4	
8	123.2	102.5	101.6	102.1	92.5	87.4	84.6	84.5	82.0	79.6	91.7	
9	135.8	112.9	111.9	112.4	101.7	96.1	93.0	92.8	90.1	87.4	100.8	
10	148.3	123.1	122.1	122.5	110.9	104.6	101.2	101.2	98.1	95.1	109.9	

4.5. Comparison of VACSIM Results to Experimental Results

A comparison between VACSIM simulations and experimental results was made for a vacuum insulated box that was filled with fumed silica. The dimensions of the box were, l=55.5cm; w=42.5cm and h=4cm and it is shown in Figure 4.29. The thicknesses of both inner and outer plastics are 3.8 mm and barrier material is ABS [11].

Figure 4.29: Vacuum insulated box

Theoretical calculations are evaluated for 21^{0}C and 25^{0}C by VACSIM-VIC program, because environmental conditions are able to change between these temperatures. The parameters used in this simulation are shown in Table 4.15. The comparison of simulation results with experimental results are given in Figure 4.30.

Table 4.15: Parameters used in VACSIM simulation for environmental conditions

V	9.435 lt
t (air)	10 year
t (WV)	10 year
P_0 (air)	0 bar
P_0 (WV)	0 bar
$P_{ff\,/\,frz}$ (air)	1.013 bar
P_{out} (air)	1.013 bar
P(25^{0}C)(WV)@%50RH	15.85 mbar
P(25^{0}C)(WV)@%50RH	15.85 mbar
T_{in}	25^{0}C
T_{out}	25 ^{0}C
A_{in}	0.236 m^2
A_{out}	0.314 m^2
T(temperature on insulation volume)	25^{0}C
$P_{sat\text{-}WVT}$@25^{0}C &50RH	15.85 mbar

The comparison of simulation results with experimental results is shown in Figure 4.30. The initial vacuum level of the vacuum insulated box was taken as 0.638 mbar, because the VIC box was evacuated until this value, after it was filled with fumed silica. A sudden increase in pressure level was observed both for experimental measurements and theoretical calculations. After this sudden increase, the pressure level starts to reach its equilibrium value. The reason of this increase is the water vapor diffusion into the insulation volume. Water vapor pressure increases rapidly until it reaches to the water vapor pressure value of the outside conditions, that is 15.83 mbar, 25^0C and 50% RH. By VACSIM simulations water vapor pressure reaches to equilibrium state in 22 hours, where it can be accepted as 16 hours for experimental measurements. After equilibrium state is reached, the pressure increase on insulation volume is only due to air diffusion. According to VACSIM results, pressure on insulation volume reaches to 100 mbar that is critical pressure value of fumed silica, in 335 days. But the conditions used for this simulation does not show the real refrigerator conditions, they only simulate the experimental conditions.

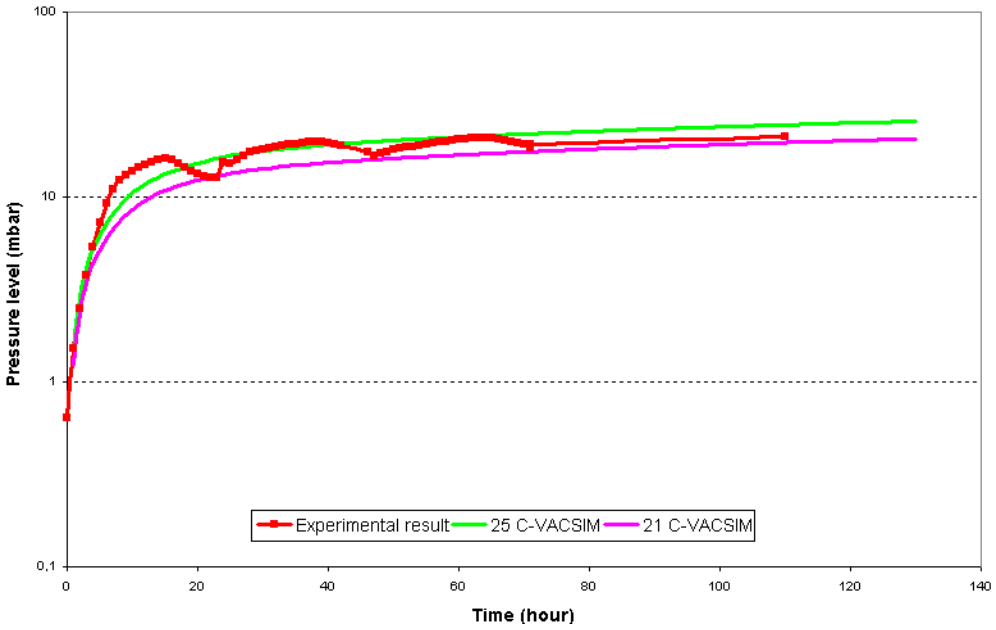

Figure 4.30: Comparison of experimental results to VACSIM simulations

This results show that theoretical results achieved by VACSIM VIC simulation program are harmonious by experimental measurements. Thus, by using VACSIM-VIC program, pressure increase in a VIC cabinet can be estimated for any desired temperature and time interval.

5.CONCLUSION AND RECOMMENDATION

In the present thesis, absorption characteristics of getter material against various gas types were investigated and the absorption performance of getter material was evaluated both by experimental measurements and theoretical calculations.

Getter shows different absorption characteristics against different gases due to the size of gas molecules and molecular interactions. Gettering capacities that were determined by experimental measurements represent minimum values. However the gettering capacities of tested getter materials are sufficient to absorb all the gases that were accumulated in the panel during its lifetime. So all the evaluated getter types have enough capacity to be used in a vacuum panel.

Pressure increases with respect to time were compared between experimental measurements and theoretical calculations both for VIP and VIC concepts. In the case of VIC concept new polymeric multilayer structures with low permeability values were suggested. Theoretical calculations that were computed by VACSIM program are very similar to the experimental results. Based on the existing evaluations, VACSIM can be used to predict vacuum level change in a period of time for any vacuum insulated system.

REFERENCES

[1] **Özkadı, F., Küçükpınar, E., Soysal, A., Özgün, S. and Güçlü, H.,** 2000. The Gas Permeability of Plastics and Evaluation Methods for Vacuum Insulated Components of Future Refrigerators, *UTECH 2000 Conference Proceeding*, Netherlands, March 28-30, 12

[2] **Çelik, A., Küçükpınar, E., Güçlü, H. and Özkadı, F.,** Analysis of adsorption characteristics of getter materials against various gases and comparison of three different types of getter, VIA 2003 Conference Proceedings, Washington, USA, May 5-6

[3] **Taşkın, D.,** 2003. Arçelik A.Ş Araştırma - Teknoloji Geliştirme Merkezi Araştırma Raporu, ARN-185, İstanbul

[4] **Comyn, J.,** 1985, Polymer Permeability, Chapman and Hall, London

[5] **Özgün, S, Güçlü H.,**1999. Arçelik A.Ş Araştırma - Teknoloji Geliştirme Merkezi Araştırma Raporu, ARN-108, İstanbul

[6] **Dr. Güçlü, H. and Özgün, S.,** 2001. Arçelik A.Ş Araştırma - Teknoloji Geliştirme Merkezi Araştırma Notu, ANN-327, İstanbul

[7] **Vacuum Insulation Association**,2003 http://www.vacuuminsulate.org/VIP_Technology

[8] **Lafferty, J.M.,**1998. Foundations of Vacuum Science and Technology, John Wiley & Sons, Inc, Canada.

[9] **Dr. Güçlü, H., Küçükpınar, E., Gönül T and Özkadı, F.,** 1998. Arçelik A.Ş Araştırma - Teknoloji Geliştirme Merkezi Araştırma Notu, ARN-96, İstanbul

[10] **Küçükpınar, E. and Dr. Güçlü, H.** 2001. Arçelik A.Ş Araştırma - Teknoloji Geliştirme Merkezi Araştırma Notu, ARN-162, İstanbul

[11] **Çelik, A. and Küçükpınar, E.,** 2002. Arçelik A.Ş Araştırma - Teknoloji Geliştirme Merkezi Araştırma Notu, ARN-204, İstanbul

[12] **Küçükpınar, E.and Özgün, S.,** 2001. Arçelik A.Ş Araştırma - Teknoloji Geliştirme Merkezi Araştırma Notu, ANN-318, İstanbul

[13] **Akkurt, S. and Özgün, S.,**1997. Arçelik A.Ş Araştırma - Teknoloji Geliştirme Merkezi Araştırma Notu, ABN-101, İstanbul

[14] **Dr. Güçlü, H. and Küçükpınar, E.,** 2001 Arçelik A.Ş Araştırma - Teknoloji Geliştirme Merkezi Araştırma Notu, ANN-315, İstanbul

[15] **Dr. Güçlü, H.,** 1999. Arçelik A.Ş Araştırma - Teknoloji Geliştirme Merkezi Araştırma Notu, ANN-202, İstanbul

[16] **Dr. Güçlü, H. and Özgün, S.,** 2001. Arçelik A.Ş Araştırma - Teknoloji Geliştirme Merkezi Araştırma Notu, ARN-158, İstanbul

[17] **Çelik, A. ve Küçükpınar, E.,**2002. Arçelik A.Ş Araştırma - Teknoloji Geliştirme Merkezi Araştırma Raporu, ARN-192, İstanbul

[18] **Manini, P.,2003.** Kişisel Görüşme

[19] **Küçükpınar, E.,Güçlü, H.,Akkurt, S. and Özkadı, F.,** 1998. Characterization of Open Cell Filler Materials for Vacuum Insulation, *SPI Polyurethanes World Congress Proceeding*, Dallas-Texas, September 17-20, 317

[20] **Manini, P.,** 1997. The COMBOGETTER^{TM} as a key component in the vacuum insulated panels (VIPs) technology, *Vuoto Vol. XXVI, N.2*, 45

[21] **Manini, P.,** 1998. Recent Developments in the Open Cell Foams-Filled Vacuum Insulated Panels for Appliances Applications, *SPI Polyurethanes World Congress Proceeding*, Dallas-Texas, September 17-20, 366

[22] **Roth, A.,** 1982. Vacuum Technology, North Holland Publishing Company, Amsterdam.

[23] **Malone B. and Weir K.,** 2001, State of the Art for VIP Usage in Refrigeration Applications, International Appliance Manufacturing,

BIOGRAPHY

Ayşe ÇELİK was born in İstanbul at 1978. She was graduated from Bahçelievler Anadolu Lisesi in 1996. She admitted to Istanbul Technical University, Chemistry Department and graduated as a chemist in 2001.

She was registered as M.Sc. student to the Polymer Science and Technology Programme of the Institute of Science and Technology of Istanbul Technical University in 2001.

She was maintained her thesis research in ARCELİK Research and Technology Development Center, Material Technologies Department in the embrace of University-Industry Cooperation.